Generation and Coupling of $[Mn(dmpe)_2(C{\equiv}CR)(C{\equiv}C)]^{\cdot}$ Radicals Producing Redox-Active C_4-Bridged Rigid-Rod Complexes

Francisco J. Fernández, Koushik Venkatesan, Olivier Blacque, Montserrat Alfonso, Helmut W. Schmalle, and Heinz Berke*[a]

Abstract: The symmetric d^5 *trans*-bis-alkynyl complexes $[Mn(dmpe)_2(C{\equiv}CSiR_3)_2]$ (R = Me, **1a**; Et, **1b**; Ph, **1c**) (dmpe = 1,2-bis(dimethylphosphino)-ethane) have been prepared by the reaction of $[Mn(dmpe)_2Br_2]$ with two equivalents of the corresponding acetylide $LiC{\equiv}CSiR_3$. The reactions of species **1** with $[Cp_2Fe][PF_6]$ yield the corresponding d^4 complexes $[Mn(dmpe)_2(C{\equiv}CSiR_3)_2][PF_6]$ (R = Me, **2a**; Et, **2b**; Ph, **2c**). These complexes react with NBu_4F (TBAF) at −10 °C to give the desilylated parent acetylide compound $[Mn(dmpe)_2(C{\equiv}CH)_2][PF_6]$ (**6**), which is stable only in solution at below 0 °C. The asymmetrically substituted *trans*-bis-alkynyl complexes $[Mn(dmpe)_2(C{\equiv}CSiR_3)(C{\equiv}CH)][PF_6]$ (R = Me, **7a**; Et, **7b**) related to **6** have been prepared by the reaction of the vinylidene compounds $[Mn(dmpe)_2(C{\equiv}CSiR_3)(C{=}CH_2)]$ (R = Me, **5a**; Et, **5b**) with two equivalents of $[Cp_2Fe][PF_6]$ and one equivalent of quinuclidine. The conversion of $[Mn(C_5H_4Me)(dmpe)I]$ with $Me_3SiC{\equiv}CSnMe_3$ and dmpe afforded the *trans*-iodide-alkynyl d^5 complex $[Mn(dmpe)_2(C{\equiv}CSiMe_3)I]$ (**9**). Complex **9** proved to be unstable with regard to ligand disproportionation reactions and could therefore not be oxidized to a unique Mn^{III} product, which prevented its further use in acetylide coupling reactions. Compounds **2** react at room temperature with one equivalent of TBAF to form the mixed-valent species $[\{Mn(dmpe)_2(C{\equiv}CH)\}_2(\mu\text{-}C_4)][PF_6]$ (**11**) by C–C coupling of $[Mn(dmpe)_2(C{\equiv}CH)(C{\equiv}C^{\cdot})]$ radicals generated by deprotonation of **6**. In a similar way, the mixed-valent complex $[\{Mn(dmpe)_2(C{\equiv}CSiMe_3)\}_2(\mu\text{-}C_4)][PF_6]$ $\mathbf{[12]^+}$ is obtained by the reaction of **7a** with one equivalent of DBU (1,8-diazabicyclo[5.4.0]undec-7-ene). The relatively long-lived radical intermediate $[Mn(dmpe)_2(C{\equiv}CH)(C{\equiv}C^{\cdot})]$ could be trapped as the Mn^I complex $[Mn(dmpe)_2(C{\equiv}CH)({\equiv}C{-}CO_2)]$ (**14**) by addition of an excess of TEMPO (2,2,6,6-tetramethyl-1-piperidinyloxy) to the reaction mixtures of species **2** and TBAF. The neutral dinuclear Mn^{II}/Mn^{II} compounds $[\{Mn(dmpe)_2(C{\equiv}CR_3)\}_2(\mu\text{-}C_4)]$ (R = H, **11**; R = $SiMe_3$, **12**) are produced by the reduction of $\mathbf{[11]^+}$ and $\mathbf{[12]^+}$, respectively, with $[FeCp(C_6Me_6)]$. $\mathbf{[11]^+}$ and $\mathbf{[12]^+}$ can also be oxidized with $[Cp_2Fe][PF_6]$ to produce the dicationic Mn^{III}/Mn^{III} species $[\{Mn(dmpe)_2(C{\equiv}CR_3)\}_2(\mu\text{-}C_4)][PF_6]_2$ (R = H, $\mathbf{[11]^{2+}}$; R = $SiMe_3$, $\mathbf{[12]^{2+}}$). Both redox processes are fully reversible. The dinuclear compounds have been characterized by NMR, IR, UV/Vis, and Raman spectroscopies, CV, and magnetic susceptibilities, as well as elemental analyses. X-ray diffraction studies have been performed on complexes **4b**, **7b**, **9**, $\mathbf{[12]^+}$, $\mathbf{[12]^{2+}}$, and **14**.

Keywords: mixed-valent compounds · molecular devices · molecular wire · nanotechnology · single-electron devices

Introduction

Organometallic polymers or oligomers consisting of dinuclear transition metal units spaced by $(\text{-}C{\equiv}C\text{-})_n$- bridges were first reported by Hagihara et al. during the late 1970s.[1–3] Even though extensive preparative explorations have supplemented this earlier work, there is still a lack of knowledge on $\text{-}(L_mM{-}C_n{-}ML_m)_n$- polymeric or oligomeric species and even on their $L_mM{-}C_n{-}ML_m$ monomers, in particular with regard to their electronic properties. NLO[4–14] and molecular wire[6,15–31] properties of complexes can often be related to their ability to undergo facile redox changes, and dinuclear and oligomeric metal μ-acetylide species are

[a] Prof. H. Berke, Dr. F. J. Fernández, Dr. K. Venkatesan, Dr. O. Blacque, Dr. M. Alfonso, Dr. H. W. Schmalle
Anorganisch-Chemisches Institut der Universität Zürich
Winterthurerstrasse 190, 8057 Zürich (Switzerland)
E-mail: hberke@aci.unizh.ch

Supporting information for this article is available on the WWW under http://www.chemeurj.org/ or from the author. Cartesian coordinates of optimized geometries, computed total bonding energies and solvation energies, magnetic susceptibility data for **12** and $\mathbf{[12]^+}$, and UV/Vis spectra of **11**, $\mathbf{[11]^+}$, and $\mathbf{[12]^{2+}}$ are given in Supporting Information.

DOI: 10.1002/chem.200305254

considered to possess such properties[12,22,32–41] on the basis of their mixed-valent states. As part of our ongoing quest for molecular electronic materials, in particular single-electron devices,[13,16,18,19,23–25,27–31,42–46] we initiated a search for dinuclear (and oligonuclear) complexes with electronically strongly coupled C_4-bridges and redox-active end-groups possessing low energy work functions and, thus, a high propensity for electron delocalization. This condition was anticipated to be reasonably well satisfied by molecular units with electron-rich phosphine-substituted manganese end-groups[47–53] and a C_4 spacer. In addition to the above reasons, the L_mMn-C_4-MnL_m systems were also selected as target molecules because the assembly of Mn di- and oligonuclear species was envisaged as being synthetically feasible not only by acetylide substitution processes, but also by the coupling of Mn–C_2 units, such as Mn–alkynyl and Mn–vinylidene moieties. Such possibilities have, in principle, been corroborated by recent studies of our group.[47–53] For instance, we have published the syntheses of redox-active dinuclear complexes of the type $\{[Mn(dmpe)_2(X)]_2(\mu\text{-}C_4)\}^{n+}$ (X = I, C≡CH, C≡C–C≡CSiMe$_3$ with n = 0–2), which were either obtained by the reaction of two equivalents of [Mn(MeCp)(dmpe)I] with Me_3Sn-C_4-$SnMe_3$ and dmpe[50] and subsequent acetylide substitution,[49] or by an in situ C–C coupling of $[Mn^{III}(dmpe)_2(C{\equiv}CH)(C{\equiv}C)]$ units[52] similar to the Eglinton and McCrae oxidative coupling of acetylenic compounds.[54] Generalization of this principal reaction path and additional insight into the reaction mechanism was expected to come from further explorations starting from suitable Mn^{III}–alkynyl complexes of the type $[Mn(dmpe)_2(C{\equiv}CSiR_3)X]^+$ (X = I, Br, C≡CSiR$_3$, C≡CH; R = Me, Et, Ph).

The Mn^{II}-species **1** can easily be oxidized with $[Cp_2Fe][PF_6]$ affording the corresponding d^4 paramagnetic $[Mn(dmpe)_2(C{\equiv}CSiR_3)_2]^+$ compounds (R = Me, **2a**;[11] Et, **2b**; Ph, **2c**) (Scheme 1). All the Mn^{III} species were isolated as red PF_6^- salts. They were found to be insoluble in alkanes, sparingly soluble in THF, but soluble in CH_2Cl_2. The ^{1}H NMR spectra of these complexes **2** show characteristic dmpe resonances at high field at around $\delta = -29.0$ and -39.0 ppm.[47–53] The $SiEt_3$ protons of **2b** give rise to two broad signals at δ = 3.70 and 2.96 ppm, and for the $SiPh_3$ protons of **2c** three broad resonances are observed at δ = 9.18, 6.98, and 6.37 ppm.

The reduction of the Mn^{II} species **1a**,**b** with sodium requires rather forcing conditions of 95 °C for more than 12 h to obtain the corresponding diamagnetic salts $[Mn(dmpe)_2(C{\equiv}CSiR_3)_2]Na$ (R = Me, **3a**;[51] Et, **3b**). In a similar fashion as for **3a**,[51] successive reaction of **3b** with MeOH afforded the corresponding Mn^I *trans*-alkynyl-vinylidene species $[Mn(dmpe)_2(C{\equiv}CSiEt_3)(C{=}CHSiEt_3)]$ (**4b**). Subsequent treatment of **4b** with MeOH/KOH led to $[Mn(dmpe)_2(C{\equiv}CSiEt_3)(C{=}CH_2)]$ (**5b**). All the new complexes **3b**, **4b**, and **5b** were fully characterized.

An X-ray study on **4b** confirmed the proposed structure (Figure 1), with the alkynyl and vinylidene ligands in a *trans* arrangement. The vinylidene C=C (1.320(7) Å) and alkynyl

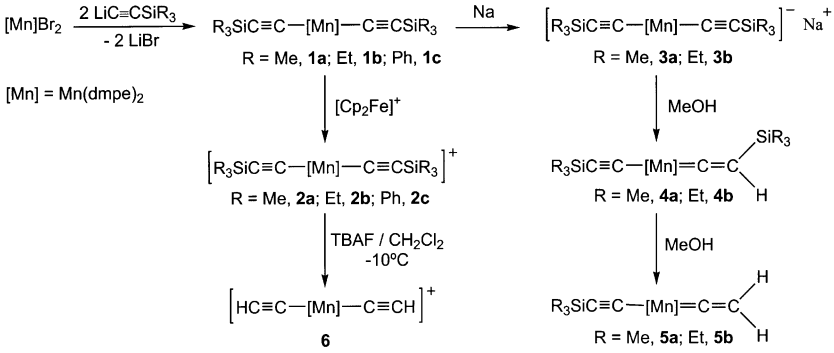

Scheme 1.

Results and Discussion

Synthesis of symmetric *trans*-bis-alkynyl manganese derivatives: Paramagnetic d^5 *trans*-bis-alkynyl manganese compounds $[Mn(dmpe)_2(C{\equiv}CSiR_3)_2]$ (R = Me, **1a**;[53] Et, **1b**; Ph, **1c**) can be prepared by the reaction of $[Mn(dmpe)_2Br_2]$ with two equivalents of $LiC{\equiv}CSiR_3$ or by the reaction of $[MnCp_2]$ (Cp = C_5H_5, C_5H_4Me) with two equivalents of $EC{\equiv}CSiR_3$ (E = H, $SnMe_3$) in the presence of dmpe.[48] Complex **1c** was previously also obtained by SiR_3 metathesis using **1a** and an excess of $[NBu_4][Ph_3F_2Si]$.[51] All these Mn^{II} *trans*-bis-alkynyl species are yellow solids. The alkyl derivatives **1a** and **1b** are much more soluble in less polar solvents, such as hexane, toluene, and Et_2O, than **1c**. The ^{1}H NMR spectrum of **1b** shows two broad signals at $\delta = -13.9$ and -15.17 ppm, corresponding to the dmpe protons. These values are characteristic for such low-spin d^5 complexes.[47–53] The $SiEt_3$ groups of **1b** give rise to two broad resonances at δ = 3.92 and 3.06 ppm.

C≡C (1.223(7) Å) bond lengths compare well with those found for the related compound **5a**.[51] There is no significant difference between the Mn–C111 (1.911(6) Å) and the Mn=C112 distances (1.891(5) Å), which might be considered as an artifact due to the statistical disorder of the alkynyl and vinylidene ligands. Nevertheless, the atom pairs C111/C112 and C211/C212, as well as C311/312 and C411/C412, could be refined in split positions with a refined site occupation ratio of 0.48/0.52.

As mentioned above, the oxidation state of the manganese center has a great influence on the reactivity of the Si–$C_{acetylene}$ bond of such *trans*-bis-alkynyl manganese derivatives. The Mn^{II}-complex **1a** does not react with TBAF at room temperature and upon heating this mixture yields decomposition products.[51] On the other hand, the Mn^{III}-species **2a–c** react instantaneously with one equivalent of TBAF even at −50 °C to produce the reactive species $[Mn(dmpe)_2(C{\equiv}CH)_2][PF_6]$ (**6**). Complex **6** could not be iso-

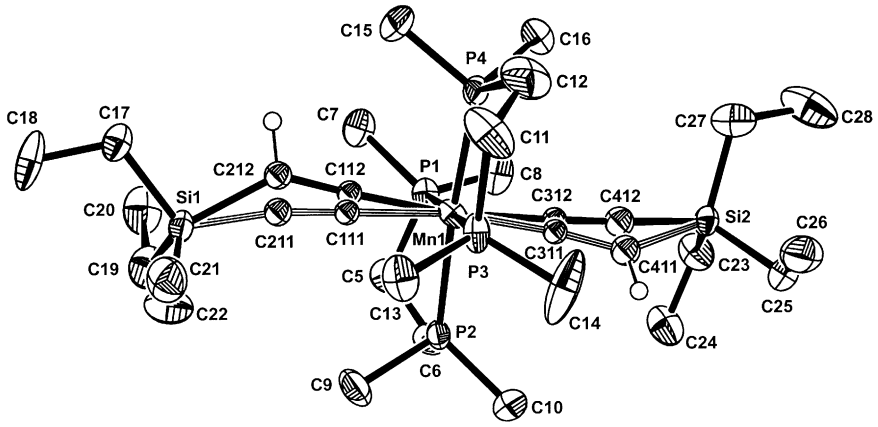

Figure 1. Molecular structure of **4b** (50% probability displacement ellipsoids). Selected bond lengths [Å] and angles [°]: Mn1–C112 1.891(5), Mn1–C312 1.894(6), Mn1–C311 1.895(7), Mn1–C111 1.911(6), Mn1–P1 2.2380(9), Mn1–P2 2.2382(9), Mn1–P3 2.2468(8), Mn1–P4 2.2405(9), Si1–C211 1.725(5), Si1–C212 1.924(5), C111–C211 1.223(7), C112–C212 1.320(7); C112-Mn1-C312 171.8(3), C112-Mn1-C311 176.7(3), C312-Mn1-C111 177.7(3), P1-Mn1-P2 84.83(3). Hydrogen atoms have been omitted for clarity, except for the vinylidene H atom. The statistical disorder is indicated by the Mn-C-C-Si three-line bond and the solid bond.

lated as a pure solid, but it is possible to store it for hours in solution at −10 °C.[52] Apart from the fact that complex **2c** is less soluble than **2a** or **2b**, no significant chemical differences were observed in these reactions with TBAF.

Synthesis of asymmetric *trans*-bis-alkynyl manganese complexes: A potential method for obtaining asymmetrically substituted Mn^{II}- or Mn^{III}-alkynyl complexes is the deprotonation of metal–vinylidene units.[55–59] We have reported the synthesis of the *trans*-alkynyl–vinylidene species $[Mn(dmpe)_2(C{\equiv}CSiMe_3)(C{=}CH_2)]$ (**5a**), prepared by desilylation of $[Mn(dmpe)_2(C{\equiv}CSiMe_3)(C{=}CHSiMe_3)]$ (**4a**);[51] both vinylidene complexes are highly basic and react instantaneously with H^+ to give the corresponding *trans*-alkynyl–carbyne compounds $[Mn(dmpe)(C{\equiv}CSiMe_3)(\equiv C{-}CH_2R)]^+$.[51] Abstraction of $H^{\cdot}$ or H^- or equivalents of these from the vinylidene moiety of **5** would allow access to asymmetric *trans*-bis-alkynyl complexes containing one Mn–C≡CH unit.

The Mn^I complexes $[Mn(dmpe)_2(C{\equiv}CSiR_3)(C{=}CH_2)]$ indeed react with one equivalent of quinuclidine and two equivalents of $[Cp_2Fe][PF_6]$ (H^- abstraction equivalent) to give the corresponding asymmetric Mn^{III} *trans*-bis-alkynyl species $[Mn(dmpe)_2(C{\equiv}CSiR_3)(C{\equiv}CH)][PF_6]$ (R = Me, **7a**; Et, **7b**) (Scheme 2). It should be mentioned that when the reaction of the vinylidene species $[Mn(dmpe)_2(C{\equiv}CSiMe_3)(C{=}CH_2)]$ was carried out with just one equivalent of $[Cp_2Fe][PF_6]$ and in the absence of a base, an inseparable mixture of the Mn^{III}-compound **7a** and the corresponding Mn^I carbyne complex[10] $[Mn(dmpe)_2(C{\equiv}CSiMe_3)(\equiv C{-}CH_3)]^+$ was obtained.

Complexes **7** have been isolated as red solids and are insoluble in pentane and sparingly soluble in THF. The ^1H NMR spectra of paramagnetic **7a** and **7b** in CD_2Cl_2 at 20 °C each feature a pair of two broad signals due to the PMe_2 protons at $\delta = -38.70/-39.80$ ppm and $\delta = -39.34/-39.80$ ppm, respectively. The appearance of non-equivalent methyl protons of the dmpe ligands confirms the axial asymmetry of these complexes. Broad resonances at $\delta = -29.50$ ppm for both **7a** and **7b** are due to the ethylene protons. Assignment of the C≡CH proton was not possible for **7a**, presumably due to overlap with the signal of the $SiMe_3$ protons, which appears as a broad resonance centered at $\delta = 7.87$ ppm. A broad singlet at $\delta = 6.69$ ppm could be attributed to the C≡CH proton of **7b**. The axial asymmetry of these species was corroborated by an exemplary X-ray study (Figure 2). The cationic moiety of **7b** shows the manganese in a pseudo-octahedral environment with the triethylsilylalkynyl and terminal alkynyl ligands in a *trans* arrangement. The Mn–C_1 and Mn–C_3 bond lengths are similar (around 1.96 Å), and are in the same range as those found for symmetric *trans*-bis-alkynyl complexes.[51,53] The C≡C bond length in the triethylsilylalkynyl ligand (1.219(7) Å) is clearly elongated in comparison with that observed for the terminal alkynyl ligand (1.181(9) Å).

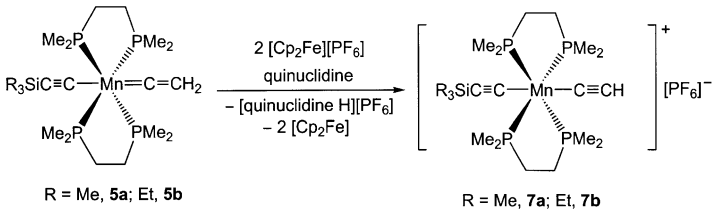

Scheme 2.

The reduction of **7a** with one equivalent of Cp_2Co yields a yellow solid, which has been identified by ^1H NMR spectroscopy as an irresolvable mixture of the Mn^{II} complexes $[Mn(dmpe)_2(C{\equiv}CSiMe_3)(C{\equiv}CH)]$ (**8a**) and (**5a**). The pure asymmetric *trans*-alkynyl Mn^{II} complex $[Mn(dmpe)_2(C{\equiv}CSiEt_3)(C{\equiv}CH)]$ (**8b**) could be obtained by reaction of **7b** with one equivalent of Cp_2Co. The ^1H NMR spectrum of **8b** in C_6D_6 shows three broad resonances at $\delta = -15.74$, -15.05, and -14.27 ppm, corresponding to the dmpe protons, and two broad signals at $\delta = 0.84$ and 1.30 ppm attributable to the $SiEt_3$ protons. The C≡CH proton gives rise to a broad resonance at $\delta = 6.69$ ppm.

Synthesis of *trans*-iodo-alkynyl manganese species: Thus far, we have described the synthesis of asymmetrically substituted *trans*-bis-alkynyl manganese complexes using manganese vinylidene complexes as starting materials. Another seemingly convenient route for obtaining the required asymmetric Mn^{II} *trans*-bis-alkynyl manganese complexes might be

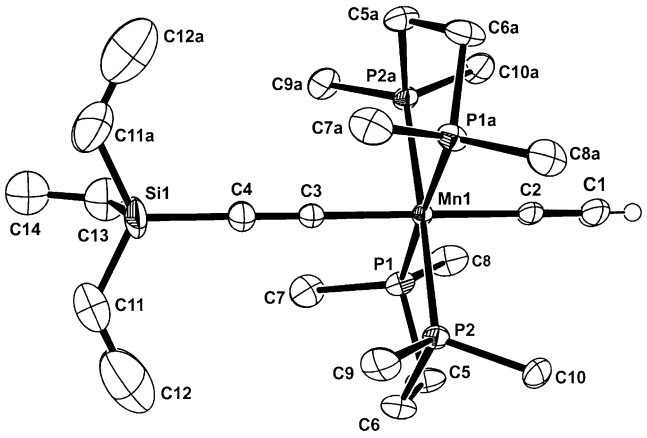

Figure 2. Molecular structure of **7b** (50% probability displacement ellipsoids). Selected bond lengths [Å] and angles [°]: Mn1–C1 1.962(5), Mn1–C3 1.965(5), Mn1–P1a 2.3195(10), Mn1–P1 2.3195(10), Mn1–P2a 2.3196(10), Mn1–P2 2.3196(10), C1–C2 1.181(9), C3–C4 1.219(7), C4–Si1 1.8122(6); C1-Mn1-C3 180, C1-Mn1-P1a 88.95(3), C3-Mn1-P1 91.05(3), P1a-Mn1-P1 177.90(7). PF_6^- counteranions and hydrogen atoms have been omitted for clarity.

envisaged as the stepwise substitution of dihalo complexes $[Mn(dmpe)_2X_2]$ (X = Br, I) through the intermediacy of appropriate monoacetylide species *trans*-$[Mn(dmpe)_2(X)(C{\equiv}CR)]$ (X = Br, I; R = H, SiR'_3). However, these *trans*-halo-alkynyl manganese compounds could not be accessed by this route, all attempts invariably leading to mixtures of the corresponding $[Mn(dmpe)_2X_2]$ (X = Br, I) and $[Mn(dmpe)_2(C{\equiv}CR)_2]$ complexes.[47]

As an alternative, conversion of the complex $[Mn(MeC_5H_4)(dmpe)I]$[60] with $[Me_3SnC{\equiv}CSiMe_3]$ and dmpe was considered, which indeed yielded the expected d^5 paramagnetic *trans*-iodo-alkynyl compound $[Mn(dmpe)_2(C{\equiv}CSiMe_3)I]$ (**9**) (Scheme 3). It could be isolated in about 40% yield as a pure red-orange solid that crystallized from pentane solution at −30 °C. The ^{1}H NMR spectrum of **9** in C_6D_6 shows two broad signals due to the dmpe protons at δ = −17.6 (PMe_2) and δ = −13.5 ppm (PCH_2), and one resonance at δ = 6.08 ppm due to the $SiMe_3$ protons.

The structure of compound **9** has been established by an X-ray diffraction study (Figure 3). The manganese center is in a pseudo-octahedral environment, with the alkynyl and iodo ligands in a *trans* arrangement. The C1–C2 and Mn–C1 distances are 1.212(4) and 1.937(3) Å, respectively. They compare well with the corresponding parameters found for $[Mn(dmpe)_2(alkynyl)_2]$ species.[47–49,51,53] The Mn-C1-C2 angle (178.9(3)°) shows a practically linear arrangement and the Mn–I distance is 2.7198(4) Å.

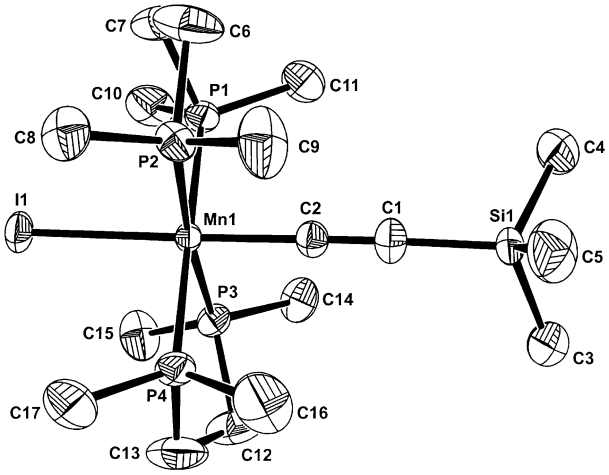

Figure 3. Molecular structure of **9** (50% probability displacement ellipsoids). Selected bond lengths [Å] and angles [°]: Mn1–C1 1.937(3), Mn1–I1 2.7198(4), Mn1–P1 2.2766(9), Mn1–P2 2.2878(9), Mn1–P3 2.2852(9), Mn1–P4 2.2897(9), C1–C2 1.212(4); C1-Mn1-I1 178.97(9), C1-C2-Si1 178.6(3), Mn1-C1-C2 178.9(3), P2-Mn1-P4 179.09(3), P1-Mn1-P3 174.22(3). Hydrogen atoms have been omitted for clarity.

When the ^{1}H NMR spectrum of pure compound **9** is recorded in C_6D_6, $[D_8]$THF or CD_2Cl_2, new signals appear after 10 minutes indicating the presence of **1a** and $[Mn(dmpe)_2I_2]$[61] (Scheme 3). Their intensities increase slowly and after 18 h at 20 °C the ligand disproportionation to these complexes is complete. This observation revealed that **9** is not sufficiently stable to expect reasonable yields in further substitutions, and its instability is presumably also responsible for the failure of the described attempts to prepare **9** by halide ligand substitution. Nevertheless, oxidation of **9** with $[Cp_2Fe][PF_6]$ was carried out in the hope of obtaining the possibly more stable and potentially more versatile $[Mn(dmpe)_2(C{\equiv}CSiMe_3)I]^+$ cation.[62] The reaction, however, afforded an irresolvable red mixture containing only minor amounts of this species. By NMR spectroscopy, **2a** and $[Mn(dmpe)_2I_2]^+$ were additionally identified.

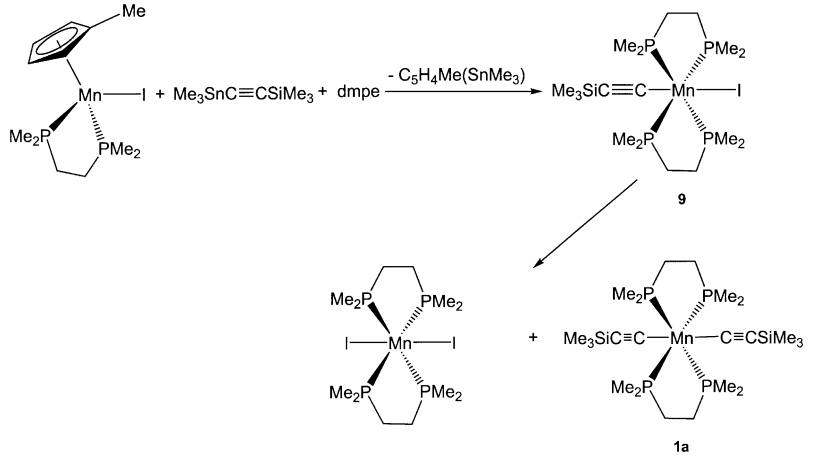

Scheme 3.

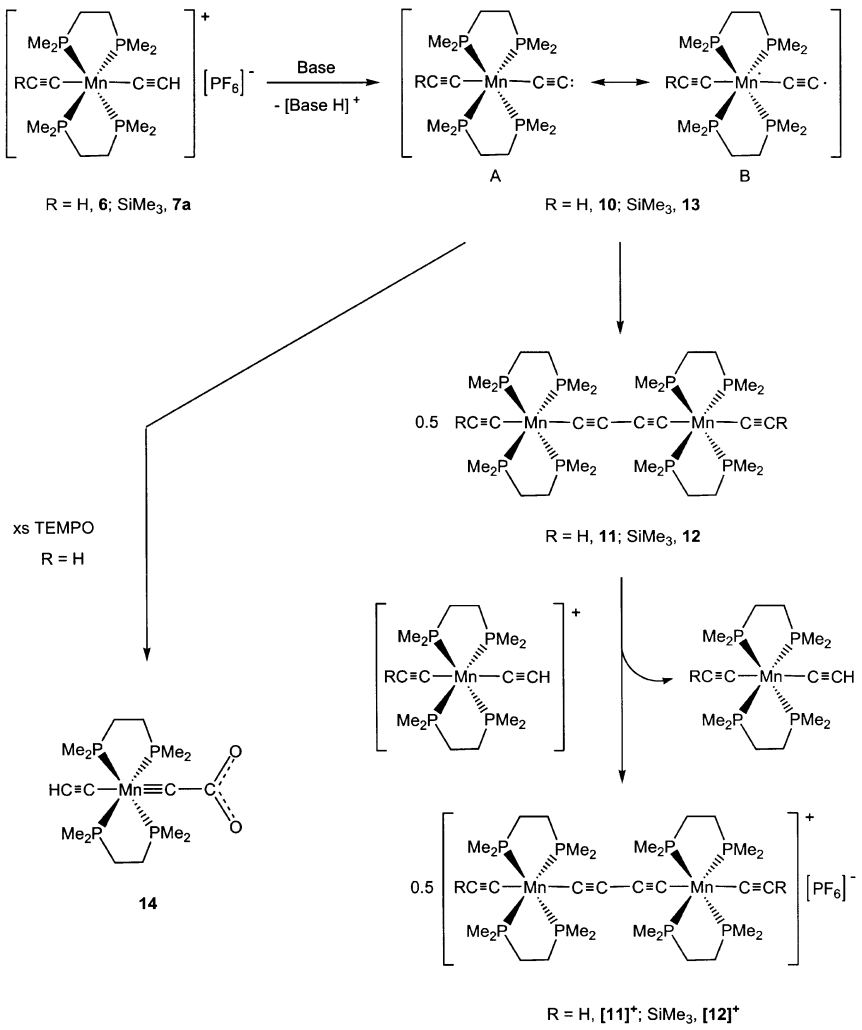

Scheme 4.

Preparation of [Mn]-C_4-[Mn] rigid-rod species: Lapinte and co-workers have reported the carbon–carbon coupling of two molecules of $[FeCp(dppe)(C{\equiv}CH)]^+$ to yield a dinuclear vinylidene species, which by subsequent deprotonation with KO*t*Bu afforded a dinuclear compound containing an Fe-C_4-Fe unit.[63] A related carbon–-carbon coupling was observed in the studies of our group using the $[Mn(MeC_5H_4)(dmpe)(C{\equiv}CPh)]$ complex.[48]

A related coupling process was considered using as starting components $[Mn(dmpe)_2(C{\equiv}CR)(C{\equiv}CH)][PF_6]$ (R = H, **6**; $SiMe_3$, **7a**). These species seemed to be sufficiently stable (**6** below −10 °C; **7a** at room temperature) and, furthermore, based on their positive charge, an initial removal of their acetylenic protons looked feasible with moderate to strong bases (DBU, F^- or OH^-) to generate the neutral "acetylides" **10** and **13**. Earlier studies revealed that, in principle, only catalytic amounts of tetrabutylammonium fluoride (TBAF) are required to desilylate Mn–C≡$CSiR_3$ units. The generation of **6** starting from **2** required one equivalent of TBAF as a desilylating agent. It should be mentioned that other related desilylations have been carried out with only catalytic amounts of TBAF.[64] F^- anions present in amounts greater than one equivalent were thought to function as a base and to induce subsequent deprotonation to give the reactive intermediate **10**. Indeed, low-temperature ^{1}H NMR studies of the reactions of **2a**, **2b** or **2c** with TBAF revealed that in each case complex **6** was formed through desilylation at −50 °C. **6** was shown to be stable in the presence of F^- for at least 1 h at −10 °C. When the temperature was finally raised to +10 °C, new resonances grew, which could be attributed to the mixed-valent complex $[\{Mn(dmpe)_2(C{\equiv}CH)\}_2(\mu\text{-}C_4)][PF_6]$ **[11]$^+$** (Scheme 4). Products of the deprotonation and coupling process could not be detected in these NMR studies. Carrying out these reactions on a preparative scale, the mixed-valent complex **[11]$^+$** was isolated as a violet solid in 65% yield starting from **2a** or **2b**, and in 37% yield from **2c**. Considering the stoichiometry of the relevant reaction steps of Scheme 4, the former yields are almost quantitative. The lower yield of **[11]$^+$** starting from **2c** can only be attributed to purification difficulties, since no differences in its reactivity were observed in the NMR studies.

In a related experiment, one equivalent of DBU was added to solutions of the asymmetric *trans*-bis-alkynyl complex **7b** in THF. Immediately after addition, a colour change from dark-red to dark-green was observed. Similarly to the reaction of **6**, the mixed-valent complex $[\{Mn(dmpe)_2(C{\equiv}CSiMe_3)\}_2(\mu\text{-}C_4)][PF_6]$ **[12]$^+$** could be isolated from these solutions in approximately 60% yield as a violet solid. The intermediacy of a species $[Mn(dmpe)_2(C{\equiv}CSiMe_3)(C{\equiv}C{:})]$ (**13**) related to **10** is proposed (Scheme 4).

Intermediates such as **10** or **13** may possess two principal canonical forms: the singlet form **A** $[Mn(dmpe)_2(C{\equiv}CR)(C{\equiv}C{:})]$ with a formally Mn^{III} center, and the triplet form **B** $[Mn(dmpe)_2(C{\equiv}CR)(C{\equiv}C^{\bullet})]$ with an oxidized C atom and a reduced Mn^{II} center. DFT calculations performed on a hydrogen-substituted model $[Mn(dHpe)_2(C{\equiv}CH)(C{\equiv}C)]$ simulating most closely **10**, but also **13**, revealed that among the two possible spin states the triplet state **B** is more stable than the singlet state by about 90 kJ mol^{-1}, and that the β-alkynyl carbon atom in the triplet state bears a substantial amount of spin density (+0.61α).[52]

The relative triplet stabilities and concomitant longevities of the Mn^{II} free radical forms of **10** and **13** enable the

selective C–C coupling process to produce initially the neutral dinuclear compounds $[\{Mn(dmpe)_2(C{\equiv}CR)\}_2(\mu\text{-}C_4)]$ (R = H, **11**; $SiMe_3$, **12**). The Mn center thus plays a similar role as the Cu^{2+} ion in the Eglinton and McCrae coupling of acetylenic compounds,[54] formally oxidizing the β-carbon atoms of terminally deprotonated species. Once **11** and **12** are formed, the given mildly oxidizing reaction conditions set by the redox properties of the Mn^{III} complexes $[Mn(dmpe)_2(C{\equiv}CR)(C{\equiv}CH)]^+$ (R = H, **6**; $SiMe_3$, **7b**) induce their subsequent oxidation to yield **[11]$^+$** and **[12]$^+$**, respectively (Scheme 4).

The ^{1}H NMR spectra of the new species **[11]$^+$** and **[12]$^+$**, recorded in CD_2Cl_2 at 20°C, each show four broad signals, at $\delta = -0.29$ (br, 8H; PCH_2), −4.60 (br, 24H; PCH_3), −6.55 (br, 24H; PCH_2), −6.71 (br, 24H; PCH_3) for **[11]$^+$**, and at $\delta = -0.26$ (PCH_2), −4.57 (PMe), −6.40 (PCH_2), and −6.50 ppm (PMe) for **[12]$^+$** (the latter two signals are overlapping). These can all be assigned to the dmpe protons. For **[12]$^+$**, an additional singlet at $\delta = 0.71$ ppm can be assigned to the $SiMe_3$ protons, while for **[11]$^+$** a signal at $\delta = -46.39$ ppm is attributable to the acetylenic proton. The only significant difference on comparing the spectra of complexes **[11]$^+$** and **[12]$^+$** is that the dmpe signals of **[12]$^+$** are slightly shifted downfield. In a quantitative fashion, the paramagnetism of **[11]$^+$** and **[12]$^+$** was confirmed by the temperature dependence of the chemical shifts, which followed Curie–Weiss behaviour (temperature range −70 to 20°C). The structure of **[12]$^+$** has been established by a single-crystal X-ray diffraction study (Figure 4). This revealed two equivalent manganese centers adopting pseudo-octahedral geometries. The bond lengths and angles compare well with those obtained for **[11]$^+$**.[52] Based on the determined carbon–carbon distances, the electronic properties of the linear C_4 chains of both compounds are best described in terms of cumulenic resonance structures.

Further support for the existence of species **10** and **13** was provided by trapping **10** with an excess of the stable nitroxide radical 2,2,6,6-tetramethyl-1-piperidinyloxyl (TEMPO). Under the given conditions, TEMPO acts as an oxygen donor[65] to form the new d^6 carboxyl–carbyne compound $[Mn(dmpe)_2(C{\equiv}CH)({\equiv}C\text{-}CO_2)]$ (**14**), which was obtained in 60% yield (NMR), together with complex **[11]$^+$** (10%) and traces of other unidentified products (Scheme 4). The corresponding reaction of **13** afforded an inseparable mixture of products. The ^{1}H NMR spectrum of this mixture suggested that complex $[Mn(dmpe)_2(C{\equiv}CSiMe_3)({\equiv}C\text{-}CO_2)]$ may have been one of its components, as indicated by a resonance at $\delta = 0.31$ ppm attributable to the $SiMe_3$ groups. The ^{31}P NMR spectrum shows a resonance at $\delta = 60.45$ ppm.

The formation of the new species **14**, and the lower yield of **[11]$^+$** obtained when an excess of TEMPO is added, support the idea of the radical nature of **10** and **13**. Despite the fact that the new complex **14** could not be isolated as a pure solid, its structure could be determined by an X-ray diffraction study since a few single crystals were separable from the impure material. The ^{1}H NMR spectrum of **14** confirms the diamagnetism of the complex, exhibiting signals due to the dmpe ligand in the range $\delta = 1.80$ to 1.10 ppm. The ^{31}P NMR spectrum of **14** shows a signal at $\delta = 60.0$ ppm, shifted somewhat to lower field with respect to the value of $\delta = 58.5$ ppm observed for the related *trans*-alkynyl–carbyne complex $[Mn(dmpe)_2(C{\equiv}CSiMe_3)({\equiv}C\text{-}CH_3)]^+$.[51]

In the structure of **14** (Figure 5), the manganese atom is in an octahedral environment, with the alkynyl and carbyne ligands in a *trans* arrangement. The C3–C4 and Mn–C3 distances are 1.216(5) and 2.060(4) Å, respectively, and compare well with those of the related $[Mn(dmpe)_2(C{\equiv}CSiMe_3)(C{=}CH_2)]$ complex.[51] The Mn-C1-C2 arrangement is linear and the Mn–C1 distance of 1.672(4) Å is similar to the Mn≡C bond length of 1.668(5) Å observed for an $[Mn({\equiv}C\text{–}C(Me){=}CPh_2)Cp(CO)(PPh_3)]^+$ species.[66] The C1–C2 bond length of 1.514(5) Å is in the range of those of C–C single bonds, while the C–O bond separations of 1.244(3) Å clearly indicate double-bond character.

Reduction of the mixed-valent complexes **[11]$^+$** and **[12]$^+$** with $[Cp(C_6Me_6)Fe]$ yields the corresponding neutral paramagnetic dinuclear species $[\{Mn(dmpe)_2(C{\equiv}CR)\}_2(\mu\text{-}C_4)]$ (R = H, **11**; $SiMe_3$, **12**), which were isolated as dark-green solids. The reactions were fully reversible and the corresponding mixed-valent species could be recovered by oxidation of the neutral complexes **11** and **12** with stoichiometric amounts

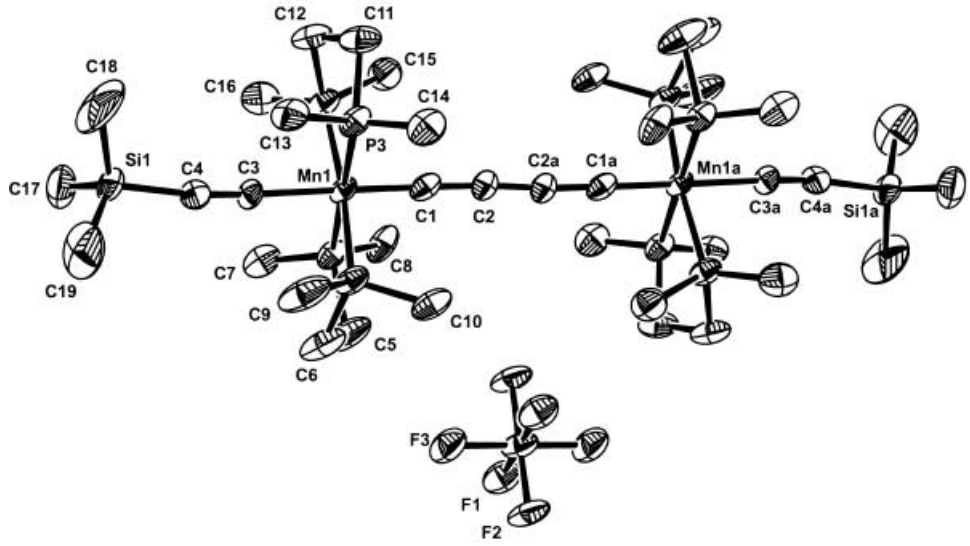

Figure 4. Molecular structure of **[12]$^+$** (50% probability displacement ellipsoids). Selected bond lengths [Å] and angles [°]: Mn1–C1 1.794(13), Mn1–C3 2.028(11), Mn1–P1 2.252(4), Mn1–P2 2.299(4), Mn1–P3 2.260(4), Mn1–P4 2.299(4), C1–C2 1.309(17), C2–C2a 1.30(2), C3–C4 1.189(15); C1-Mn1-C3 178.8(5), C3-C4-Si1 171.9(10), P2-Mn1-P4 179.00(16), P1-Mn1-P3 179.63(18). Hydrogen atoms have been omitted for clarity.

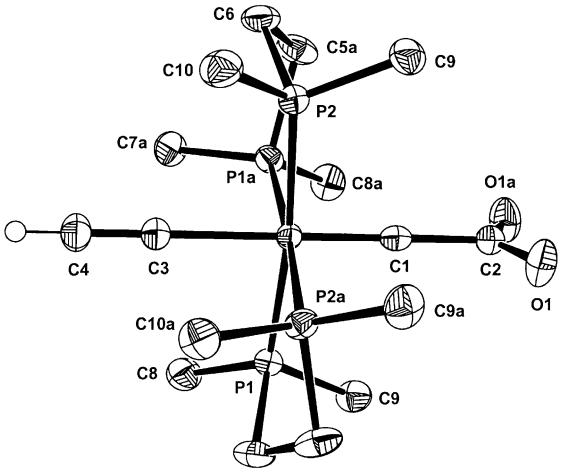

Figure 5. Molecular structure of **14** (50% probability displacement ellipsoids). Selected bond lengths [Å] and angles [°]: Mn1–C1 1.672(4), Mn1–C3 2.060(4), Mn1–P1 2.2817(7), Mn1–P2 2.2806(6), C1–C2 1.514(5), C3–C4 1.216(5), C2–O1 1.244(3); C1-Mn1-C3 180, C1-C2-O1 114.99(17), O1-C2-O1a 130.0(3), Mn1-C1-C2 180, P1-Mn1-P1a 176.19(5), P2-Mn1-P2a 173.41(5). Hydrogen atoms and the toluene solvate molecule have been omitted for clarity.

of $[Cp_2Fe][PF_6]$. The ^1H NMR spectra of the complexes **11** and **12**, recorded in C_6D_6 at 20°C, show four signals for each complex, at $\delta = -9.47$ (br, 8H; PCH_2), -14.89 (br, 32H; $PMe_3 + PCH_2$), -18.78 ppm (br, 24H; PCH_3) for **11**, and at $\delta = -10.42$ (PCH_2), -15.83 (PCH_2), -16.43 (PMe), and -20.34 ppm (PMe) for **12**, attributable to the dmpe protons. The signal of the $H_{acetylide}$ nucleus of **11** appears at $\delta = -149.4$ ppm and the $SiMe_3$ resonance of **12** is observed at $\delta = 2.85$ ppm, both shifted due to the paramagnetism of the compounds.

The redox-active mixed-valent complexes **[11]$^+$** and **[12]$^+$** can also be oxidized further to the dicationic species **[11]$^{2+}$** and **[12]$^{2+}$** by applying one equivalent of $[Cp_2Fe][PF_6]$. **[11]$^{2+}$** and **[12]$^{2+}$** are brown diamagnetic solids. Both compounds are soluble only in polar solvents such as THF and CH_2Cl_2. The ^1H NMR spectra of **[11]$^{2+}$** and **[12]$^{2+}$** in CH_2Cl_2 show resonances of the dmpe ligand in the diamagnetic region at $\delta = 1.92$ (PCH_2), 1.40 (PMe), and 1.32 ppm (PMe). Additional resonances are observed for **[12]$^{2+}$** at $\delta = -0.14$ ppm due to the $SiMe_3$ protons and for **[11]$^{2+}$** at $\delta = 2.30$ ppm due to the acetylide H atoms. The diamagnetism of the Mn^{III}-C_4-Mn^{III} species **[11]$^{2+}$** and **[12]$^{2+}$** is in agreement with the magnetic properties described for related iodo-substituted complexes.[50,52] In a similar fashion as described for the species **[11]$^+$** and **[12]$^+$**, complexes **[11]$^{2+}$** and **[12]$^{2+}$** could be re-reduced using $Cp(C_6Me_6)Fe$ to afford **[11]$^+$** and **[12]$^+$**. All redox steps are therefore fully reversible.[52] The mixed-valent species **[11]$^+$** or **[12]$^+$** could be recovered in 100% yield from the comproportionation reaction of the corresponding Mn^{III}-C_4-Mn^{III} complex **[11]$^{2+}$** or **[12]$^{2+}$** with equimolar amounts of the Mn^{II}-C_4-Mn^{II} species **11** or **12** (Scheme 5). The CV results to be discussed later confirm in a quantitative fashion that these equilibria lie fully on the side of the comproportionation products.

The structure of complex **[12]$^{2+}$** has been additionally confirmed by a single-crystal X-ray diffraction study

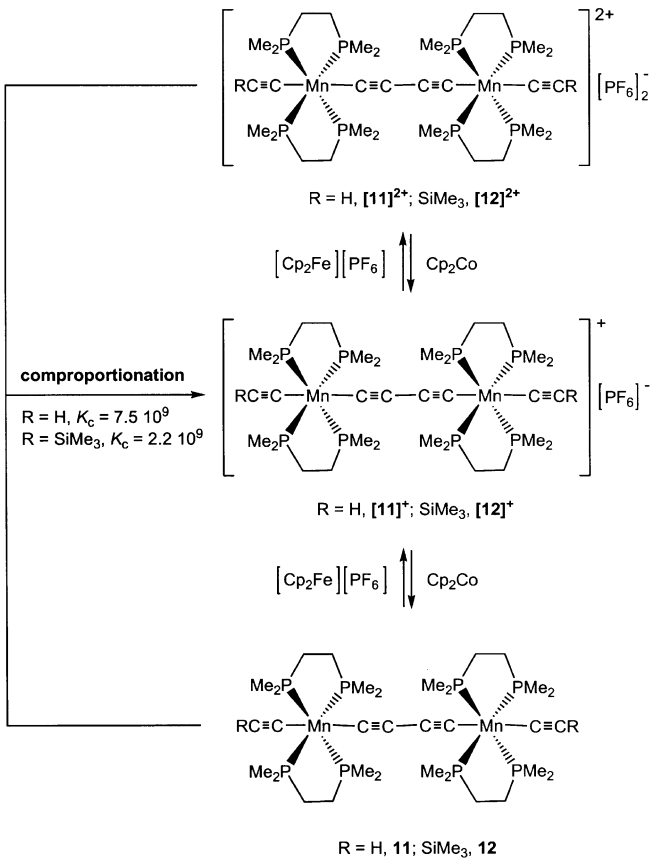

Scheme 5.

(Figure 6). This revealed two equivalent manganese centers adopting pseudo-octahedral geometries. The Mn···Mn distance in **[12]$^{2+}$** is 7.42 Å, somewhat shorter than the value of 7.50 Å observed for the complex **[12]$^+$**. A related dependence of the Mn···Mn distance on the oxidation states of the manganese centers was observed in the series of complexes $[\{Mn(dmpe)_2I\}_2(\mu\text{-}C_4)]^{n+}$ ($n = 0, 1, 2$).[49]

Physical studies (Raman, UV/Vis, EPR spectroscopy, cyclic voltammetry (CV) and magnetic susceptibility) on the dinuclear species 11, 12, [11]$^+$, [12]$^+$, [11]$^{2+}$, and [12]$^{2+}$: Due to the local D_{2h} symmetry of the species **11**, **12**, **[11]$^+$**, **[12]$^+$**, **[11]$^{2+}$**, and **[12]$^{2+}$**, with a center of inversion, bands assigned to symmetric vibrations of the C_4 chain are expected to be Raman-allowed. Symmetric bond-stretching vibrations (a_{1g}) should appear as strong bands and, indeed, the solid-state Raman spectra of these dinuclear complexes exhibit an intense and characteristic band at $\tilde{\nu} \approx 1800\ cm^{-1}$, with a shoulder at $\tilde{\nu} \approx 1830\ cm^{-1}$ for the Mn^{II}-C_4-Mn^{II} compounds **11** and **12**, at $\tilde{\nu} \approx 1750\ cm^{-1}$ for the mixed-valent complexes **[11]$^+$** and **[12]$^+$**, and at $\tilde{\nu} \approx 2000\ cm^{-1}$ for the diamagnetic species **[11]$^{2+}$** and **[12]$^{2+}$** (Figure 7; Table 1). These emissions indeed correspond to a_{1g} vibrations of the C_4 chain.[4,5,8,67–70] The observed shifts of the $\tilde{\nu}(C_4)$ bands indicate significant changes in the electronic configuration of the C_4 chain upon oxidation of the metal center(s). This behaviour is typical of strongly electronically coupled systems, and is also reflected in the X-ray studies of the complexes

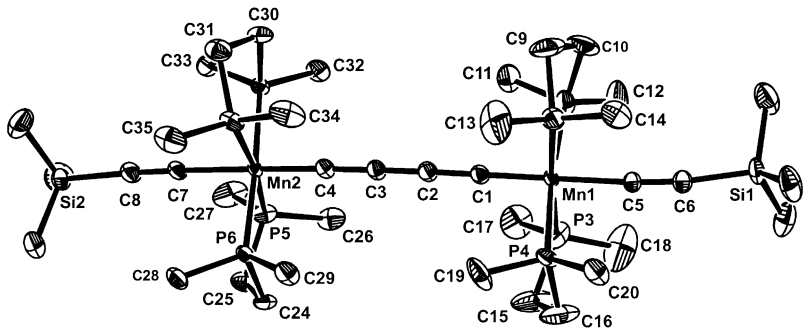

Figure 6. Molecular structure of $[12]^{2+}$ (50% probability displacement ellipsoids). Selected bond lengths [Å] and angles [°]: Mn1–C1 1.776(4), Mn1–C5 1.998(4), Mn1–P2 2.2948(12), Mn1–P3 2.2926(12), Mn2–C4 1.769(4), Mn2–C7 1.993(4), C1–C2 1.292(5), C2–C3 1.282(5), C3–C4 1.302(5), C5–C6 1.211(5), C7–C8 1.222(5); C1-Mn1-C5 179.07(17), Si1-C6-C5 177.1(4), C1-C2-C3 179.6(4), C2-C3-C4 178.9(4) C4-Mn2-C7 179.49(16), C7-C8-Si2 171.9(3). Hydrogen atoms, PF_6^- counteranions, and the THF solvate molecule have been omitted for clarity.

Table 1. Raman data [cm^{-1}] for compounds **7**, **8**, **11**, **12**, $[11]^+$, and $[12]^+$.

	7	8	$[11]^+$	$[12]^+$	11	12
C≡C (weak)	2157	2130				
C≡C (weak)	1902	1986	1830	1820		
C≡C (a_{1g})	1732	1748	1800	1799	1931	2006
C–C–C	1033	1043	1043	1050	1050	1048
Mn–C	414	371	345	423	406	354
Mn–P (weak)	276	250	[a]	[a]	257	[a]

[a] Not observed.

The oxidations of the neutral molecules **12** and **11** occur at relatively negative absolute potentials, suggesting loosely bound electrons (low energy work functions) in energetically high-lying HOMOs. Furthermore, the oxidation of **12** with the more strongly coupled Mn centers occurs at a still more negative potential (−0.816 V) than that of **11** (−0.451 V). DFT calculations, including simulations of solvation effects on the model systems $[\{Mn(dHpe)_2R\}_2(\mu\text{-}C_4)]^{n+}$ (n = 0, 1, 2; R = C≡CH, C≡C–$SiMe_3$), confirm energetically high-lying HOMOs for the neutral compounds at −3.40 eV (R = C≡CH) and at −3.47 eV (R = C≡C–$SiMe_3$) (see Supporting Information). The triplet state of the neutral compounds is preferred over the singlet state

$[11]^+$,[52] $[12]^+$, and $[12]^{2+}$, and of the $[\{Mn(dmpe)_2I\}_2(\mu\text{-}C_4)]^{n+}$ series (n = 0, 1, 2).[50] Other relevant bands in these spectra are $\tilde{\nu}(C_3)$ vibrations of the C_4 chain,[5] which appear at around $\tilde{\nu} \approx 1040\ cm^{-1}$. In addition, an emission at around 340 cm^{-1} is assigned to the Mn–C vibration for all complexes,[71] and a band at around 270 cm^{-1} is attributed to a_{1g} Mn–P stretching vibrations.[72]

The cyclic voltammograms (CV, at 20 °C, NBu_4PF_6/THF, gold electrode, vs Fc/Fc^+) (Figure 8) of complexes **12**, $[12]^+$, and $[12]^{2+}$ display two fully reversible waves, one at $E_{1/2}$ = −0.816 V corresponding to the Mn^{II}-C_4-Mn^{III} ($[12]^+$)/Mn^{II}-C_4-Mn^{II} (**12**) redox couple (ΔE_p = 0.060 V and $i_{pa}/i_{pc} \approx 1$ for scan rates of 0.100–0.700 $V\,s^{-1}$), and the other at $E_{1/2}$ = −0.271 V due to the Mn^{III}-C_4-Mn^{III} ($[12]^{2+}$)/Mn^{III}-C_4-Mn^{II} ($[12]^+$) couple. The difference of these values of $\Delta E_{1/2}$ = 0.545 V establishes a comproportionation constant of 2.2×10^9 ($K_c = \exp(F\Delta E_{1/2}/RT)$).[73a] Additionally, we can observe a small peak attributable to the formation of an Mn^{IV}-C_4-Mn^{III} species, which, once it is produced, decomposes at the electrode surface in the course of the experiment. The CV of the **11**/$[11]^+$/$[11]^{2+}$ system (Figure 9) displays two reversible waves at $E_{1/2}$ = −0.451 V and $E_{1/2}$ = +0.124 V, corresponding to the Mn^{III}–Mn^{II} ($[11]^+$)/Mn^{II}–Mn^{II} (**11**) and Mn^{III}–Mn^{III} ($[11]^{2+}$)/Mn^{III}–Mn^{II} ($[11]^+$) redox couples, respectively. The difference of these two values of $\Delta E_{1/2}$ = 0.575 V establishes a comproportionation constant K_c of 7.5×10^9.[52] The value of K_c obtained for $[12]^+$ (2.2×10^9) is somewhat lower than that obtained for complex $[11]^+$ and indeed represents a value at the lower end of the range for the series of $[\{Mn(dmpe)_2(X)\}_2(\mu\text{-}C_4)]^{n+}$ complexes (X = I, 1.1×10^{10}; X = C≡CH, 7.5×10^9; X = C≡CSiMe_3, 2.2×10^9; X = C_4–SiMe_3, 1.8×10^8).[49,50,52]

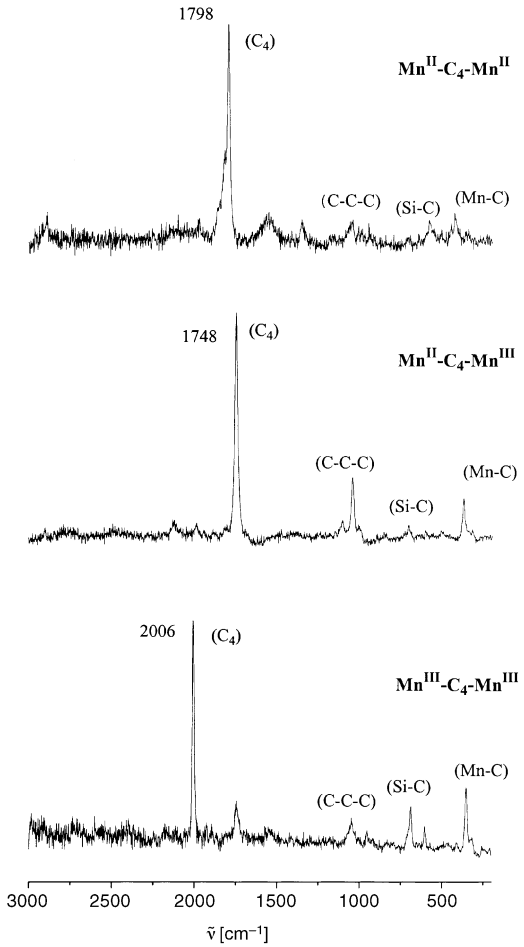

Figure 7. Solid-state Raman spectra of the complexes **12**, $[12]^+$, and $[12]^{2+}$; incident laser at 514 nm.

by about 0.33 eV (32 kJ mol^{-1}) for both models, while the ground states of mono- and dicationic species have been found as low-spin configurations with one and zero unpaired electrons, respectively. Unfortunately, a theoretical interpretation of the first oxidation of **12** compared to **11** based on their HOMO energies and/or computed gas-phase first ionization potentials IP_1 failed ($IP_1 = E_{tot}(model^+) - E_{tot}(model) = 4.25$ and 4.28 eV for R = C≡CH and R = C≡C–$SiMe_3$, respectively). Nevertheless, the lower IP_2 calculated for the mixed-valent compound **[12]$^+$** ($IP_2 = E_{tot}(model^{2+}) - E_{tot}(model^+) = 5.81$ vs 5.87 eV for **[11]$^+$**, leading to $\Delta IP = IP_2 - IP_1 = 1.53$ vs 1.62) is suggestive of a greater stability of **[11]$^+$**. These values correlate well with the experimentally measured $\Delta E_{1/2}$ potentials (0.575 and 0.545 V for R = C≡CH and R = C≡C–$SiMe_3$, respectively). Further calculations performed on the series $[\{Mn(dHpe)_2I\}_2(\mu\text{-}C_4)]^{n+}$ (n = 0, 1, 2) showed a lower-lying HOMO at −3.77 eV for the neutral compound compared to the models with H and $SiMe_3$. The calculated highest value of 4.57 eV for IP_1 confirms that the corresponding unpaired electron is more difficult to remove from the molecule, thus accounting for the fact that the first oxidation wave is shifted to more positive potentials (−0.210 V). However, the parameter ΔIP introduced by Floriani et al.[74] to give a theoretical estimate of the metal–metal interaction in the case of $[\{Cp(CO)_2Fe\}_2(\mu\text{-}C_n)]$ (n = 2, 4, 6, 8) seems to be inappropriate to study the ligand influences, at least in the given dinuclear manganese systems. Indeed, although there is good agreement in the trends of the parameters ΔIP and $\Delta E_{1/2}$, the difference between the values found for R = C≡CH and R = I (1.62 and 1.63, respectively) seems too small to be significant.

While the $\Delta E_{1/2}$ values provide equilibrium data, that is, thermodynamic data, on the basis of which the electronic coupling of mixed-valent metal centers could be assessed, EPR spectra of the mixed-valent species may sometimes offer kinetic estimates of the rates of the electron "movement" between the metal centers.[75–81] An EPR spectrum of **[12]$^+$** recorded at 10 K in CH_2Cl_2/EtOH glass shows a broadened signal due to a single electron at H = 3340 G with g = 2.010. However, the ^{55}Mn hyperfine coupling was only faintly recognizable and not really resolved, so that no conclusion as to whether there is coupling to both or just to one Mn center could be drawn.

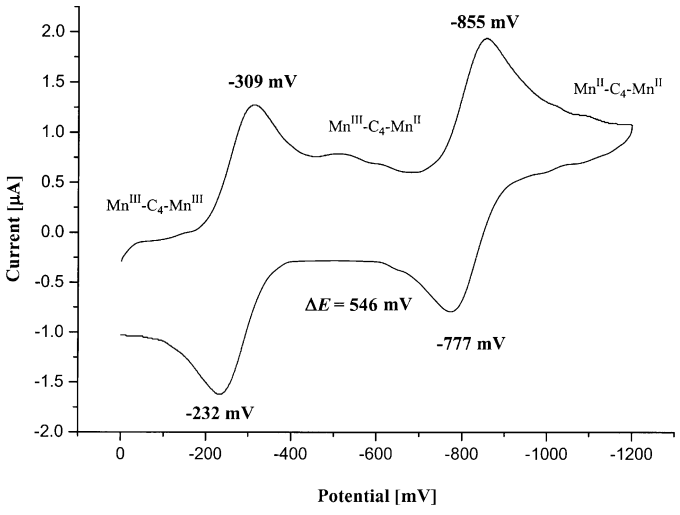

Figure 8. Cyclic voltammogram of **[12]$^+$** (10^{-3} M in nBu$_4$NPF$_6$/THF; vs Fc/Fc$^+$; Au electrode; 100 mV s^{-1}).

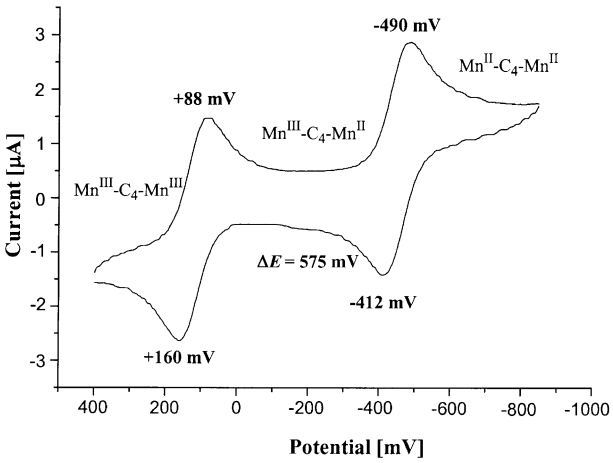

Figure 9. Cyclic voltammogram of **11** (10^{-3} M in nBu$_4$NPF$_6$/THF; vs Fc/Fc$^+$; Au electrode; 100 mV s^{-1}).

UV/Vis spectra of the series of complexes **11**, **[11]$^+$**, and **[11]$^{2+}$**, and **12**, **[12]$^+$**, and **[12]$^{2+}$**, have been recorded, which are well-structured and show two intense bands in each case. For **[11]$^+$**, **[11]$^{2+}$**, **[12]$^+$**, and **[12]$^{2+}$**, one additional band of low intensity is also observed at shorter wavelength. In comparison with the spectra of **11** and **[11]$^{2+}$**, and **12** and **[12]$^{2+}$**, respectively, **[11]$^+$** and **[12]$^+$** do not show an extra broad absorption at the long-wavelength end that could be assigned to a mixed-valence band,[32,36,73,82–96] as expected for class II systems according to the Robin–Day classification. In accord with the CV results, this allows us to conclude that the manganese end-groups of **11**, **[11]$^+$**, and **[11]$^{2+}$**, and of **12**, **[12]$^+$**, and **[12]$^{2+}$**, are electronically strongly coupled and that these complexes belong to class III. Furthermore, it is quite remarkable to see how strongly the systems are affected by charge, since the two major transitions, which are expected to arise from the same types of orbitals,[97] shift to shorter wavelengths on going from **11** to **[11]$^+$**, or from **12** to **[12]$^+$** (Figure 10). This is presumably due to the filled orbitals in the HOMO region of **11** or **12**, which are particularly sensitive to positive charge and are therefore significantly lowered in energy.

The temperature-dependent magnetic susceptibilities have been studied for all three complexes in each series **11**, **[11]$^+$**, and **[11]$^{2+}$**, and **12**, **[12]$^+$**, and **[12]$^{2+}$**. Compounds **[11]$^{2+}$** and **[12]$^{2+}$** revealed diamagnetic behaviour, as had already been indicated by NMR spectroscopy, while **[11]$^+$** and **[12]$^+$** showed paramagnetism with Curie–Weiss behaviour (Figure 11). Compound **11** has a magnetic moment of 2.53 μ_B at 290 K that drops to 1.95 μ_B at 100 K, while **12** has a value of 1.78 μ_B at 200 K that drops to 1.39 μ_B at 5 K, demonstrating antiferromagnetic interactions comparable to that observed for $[\{Mn(dmpe)_2I\}_2(\mu\text{-}C_4)]$.[32,36,50,96,98–100]

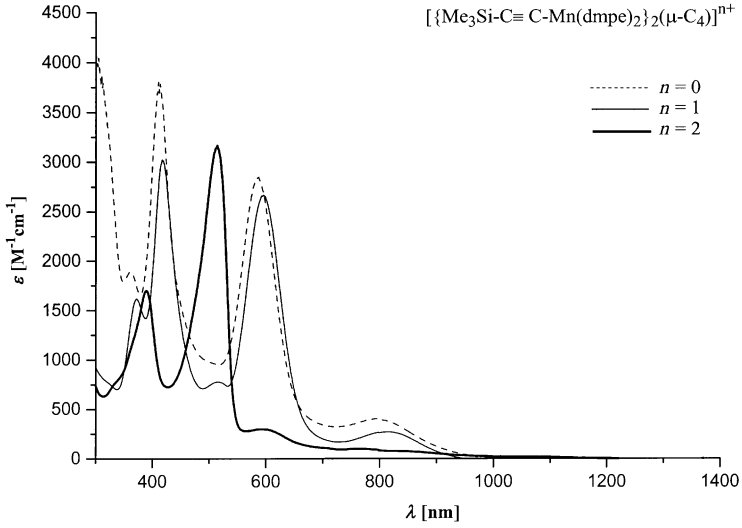

Figure 10. UV/Vis spectra of **12**, **[12]$^+$**, and **[12]$^{2+}$** (CH_2Cl_2, ambient temperature, 1×10^{-4} M).

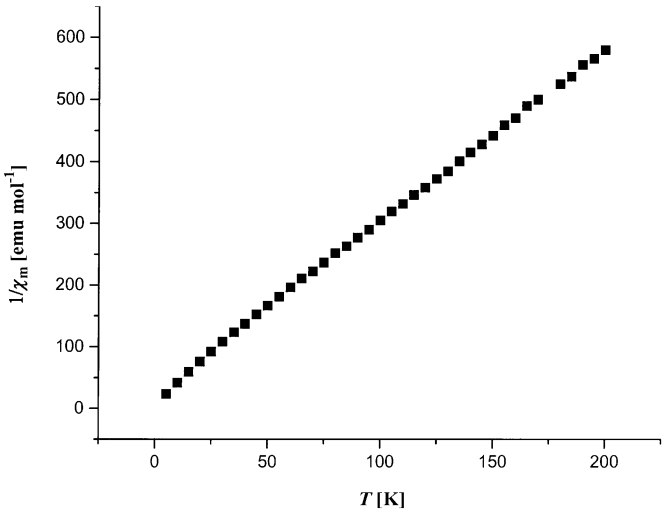

Figure 11. Temperature dependence of the reciprocal molar magnetic susceptibility for **[12]$^+$**.

Conclusion

A series of Mn^{II} and Mn^{III} symmetric and asymmetric *trans*-bis-alkynyl complexes of the type $[Mn(dmpe)_2(C{\equiv}CSiR_3)_2]^{n+}$ (R = Me, Et, Ph) and $[Mn(dmpe)_2(C{\equiv}CSiMe_3)(C{\equiv}CH)]^{n+}$ (n = 0, 1) has been prepared. The reactions of the symmetrically substituted *trans*-bis-alkynyl d^4 manganese complexes with one equivalent of TBAF at −10 °C produce the desilylated complex $[Mn(dmpe)_2(C{\equiv}CH)_2]^+$ (**6**), which at room temperature is transformed into the mixed-valent species $[\{Mn(dmpe)_2(C{\equiv}CH)\}_2(\mu\text{-}C_4)][PF_6]$ (**[11]$^+$**). The asymmetric *trans*-bis-alkynyl complex $[Mn(dmpe)_2(C{\equiv}CSiMe_3)(C{\equiv}CH)]^+$ (**7a**), which is obtained by the reaction of the Mn^I *trans*-alkynyl–vinylidene species $[Mn(dmpe)_2(C{\equiv}CSiMe_3)(C{=}CH_2)]$ with quinuclidine, reacts in the presence of two equivalents of $[Cp_2Fe][PF_6]$ and one equivalent of DBU to yield the mixed-valent complex $[\{Mn(dmpe)_2(C{\equiv}CSiMe_3)\}_2(\mu\text{-}C_4)][PF_6]$ (**[12]$^+$**), and thus, to a certain extent, suggests generality for such coupling processes.

The formation of the new dinuclear mixed-valent species **[11]$^+$** and **[12]$^+$**, recovered following the deprotonation of the corresponding terminal alkynyl manganese complexes, are unique examples of radical C–C self-coupling reactions, in which the Mn^{III} center may be considered to oxidize C_β of the deprotonated alkynyl species (**10** or **13**) generating a free radical center and subsequently inducing the C–C coupling. The coupling of these radical species is almost totally suppressed when these reactions of the species **2** with TBAF are carried out in the presence of TEMPO. It was thus possible to trap the intermediates through the formation of the unique compound $[Mn(dmpe)_2(C{\equiv}CH)(\equiv C{-}CO_2)]$ (**14**). Several types of physical studies on the obtained dinuclear compounds indicate that they all show strong electronic coupling of the manganese centers according to class III systems of the Robin–Day classification. There is a noticeable substituent effect, since for the silyl-substituted complexes **12**, **[12]$^+$**, and **[12]$^{2+}$**, the coupling is less pronounced than that in the parent H species **11**, **[11]$^+$**, and **[11]$^{2+}$**. This has been rationalized on the basis of DFT calculations.

Experimental Section

General: All operations were performed under an inert atmosphere of N_2 using Schlenk and vacuum-line techniques or in a glove box, model MB-150B-G. The following solvents were dried and purified by distillation under nitrogen before use, employing appropriate drying/deoxygenating agents: tetrahydrofuran (sodium/benzophenone), toluene (sodium) and hexane (sodium/potassium alloy), CH_2Cl_2 (P_2O_5, with filtration through active Alox). IR spectra were obtained on a Bio-Rad FTS instrument. Raman spectra were recorded on a Renishaw Ramanscope spectrometer (514 nm). ESR measurements were made on a Bruker ER-200 instrument. Magnetic susceptibilities were measured on MPMS-5S and PPMS-6000 instruments. NMR spectra were recorded on Unity 300 or Varian Gemini 200 spectrometers at 300 or 200 MHz, respectively, for ^1H. The assignment of the ^1H NMR signals of paramagnetic compounds has been principally based on the investigations of Köhler et al.[60] Chemical shifts for ^1H NMR are reported in ppm units with respect to the signals of residual protons in the solvents. C and H elemental analyses were performed with a LECO CHN-932 microanalyzer. Cyclic voltammograms were obtained with a BAS 100 B/W instrument (10^{-3} M in 0.1 M $[NBu_4][PF_6]$ in THF; AgO reference electrode). TBAF, TEMPO, DBU, and quinuclidine were obtained from Aldrich. $[Mn(dmpe)_2Br_2]$,[61] **5a**,[51] **1a**, and **2a**[53] were prepared according to literature procedures.

Synthesis of $[Mn(dmpe)_2(C{\equiv}CSiEt_3)_2]$ (1b): A solution of freshly prepared $LiC{\equiv}CSiEt_3$ (0.39 mmol) in THF (5 mL) was added to a solution of $[Mn(dmpe)_2Br_2]$ (100 mg, 0.19 mmol) in THF at −30 °C. The temperature was raised to 20 °C and the mixture was stirred for 10 h. The solvent was removed in vacuo and the yellow solid of **1b** was extracted with hexane (100 mg, 84 %). ^1H NMR (C_6D_6, 300 MHz, 20 °C): δ = 3.92 (br, 12H; $SiEt_3$), 3.06 (br, 18H; $SiEt_3$), −13.9 (br, 8H; PCH_2), −15.17 (br, 24H; PCH_3); IR (CH_2Cl_2, 20 °C): $\tilde{\nu}$ = 1942 cm^{-1} (ν(C≡C)); elemental analysis calcd (%) for $C_{28}H_{62}P_4Si_2Mn$ (633.8): C 53.06, H 9.86; found: C 52.88, H 10.17.

Synthesis of $[Mn(dmpe)_2(C{\equiv}CSiPh_3)_2]$ (1c): A solution of freshly prepared $LiC{\equiv}CSiPh_3$ (0.39 mmol) in THF (5 mL) was added to a solution of $Mn(dmpe)_2Br_2$ (100 mg, 0.19 mmol) in THF at −30 °C. The temperature was raised to 20 °C and the mixture was stirred for 10 h. The solvent was removed in vacuo. After extraction with hexane and removal of the

solvent, **1c** (100 mg, 60%) was obtained as a yellow solid. The IR and NMR spectra of **1c** were in agreement with literature data.[51]

Synthesis of [Mn(dmpe)$_2$(C≡CSiEt$_3$)$_2$][PF$_6$] (2b): A solution of **1b** (110 mg, 0.17 mmol) in CH_2Cl_2 was added to a suspension of [Cp$_2$Fe][PF$_6$] (60 mg, 0.18 mmol) in the same solvent. After 1.5 h, the mixture was concentrated and Et_2O (10 mL) was added to afford a red precipitate of **2b** (100 mg, 80%). ^{1}H NMR (CD_2Cl_2, 300 MHz, 20°C): δ = 3.70 (br, 12H; SiEt$_3$), 2.96 (br, 18H; SiEt$_3$), −29.33 (br, 8H; PCH$_2$), −39.36 (br, 24H; PCH$_3$); ^{31}P NMR (20°C, CD_2Cl_2, 121.5 MHz): δ = −145.5 (sept, J = 718 Hz, 1P; PF$_6$); ^{19}F NMR (CD_2Cl_2, 282.32 MHz, 20°C): δ = −75.4 (d, J = 718 Hz, 6F; PF$_6$); elemental analysis calcd (%) for $C_{28}H_{62}F_6P_5Si_2Mn$ (778.8): C 43.18, H 8.02; found: C 42.91, H 7.89.

Synthesis of [Mn(dmpe)$_2$(C≡CSiPh$_3$)$_2$][PF$_6$] (2c): A solution of **1c** (150 mg, 0.17 mmol) in CH_2Cl_2 (10 mL) was added to a suspension of [Cp$_2$Fe][PF$_6$] (60 mg, 0.18 mmol) in the same solvent (5 mL). After 1.5 h, the mixture was concentrated and Et_2O (10 mL) was added. A red precipitate of **2c** was obtained (140 mg, 80%). ^{1}H NMR (CD_2Cl_2, 300 MHz, 20°C): δ = 9.21 (br, 12H; SiPh$_3$), 7.00 (br, 12H; SiPh$_3$), 6.35 (br, 6H; SiPh$_3$), −29.70 (br, 8H; PCH$_2$), −38.60 (br, 24H; PCH$_3$); ^{31}P NMR (CD_2Cl_2, 121.5 MHz, 20°C): δ = −145.3 (sept, J = 718 Hz, 1P; PF$_6$); ^{19}F NMR (CD_2Cl_2, 282.32 MHz, 20°C): δ = −75.3 (d, J = 718 Hz, 6F; PF$_6$); elemental analysis calcd (%) for $C_{52}H_{62}F_6MnP_5Si_2$ (1067.0): C 58.53, H 5.86; found: C 58.21, H 5.86.

Synthesis of [Mn(dmpe)$_2$(C≡CSiEt$_3$)$_2$]Na (3b): A solution of **1b** (420 mg, 0.74 mmol) in toluene (15 mL) was added to a large excess of sodium placed in a high-vacuum Schlenk tube fitted with a Teflon tap. The mixture was stirred at 95°C for 12 h to give a dark-red solution. This solution was then concentrated in vacuo to a volume of 5 mL and chilled at −30°C for 12 h to afford yellow crystals of complex **3b** (360 mg, 80%). ^{1}H NMR ($C_6D_5CD_3$, 300 MHz, 20°C): δ = 1.53 (s, 6H; PMe$_2$), 1.43 (m, 4H; PCH$_2$), 1.36 (s, 6H; PMe$_2$), 1.23 (s, 6H; PMe$_2$), 1.10 (m, 4H; PCH$_2$), 1.06 (t, 18H; SiCH$_2$C*H*$_3$), 0.91 (s, 6H; PMe$_2$), 0.51 (q, 12H; SiC*H*$_2$CH$_3$); ^{31}P NMR ($C_6D_5CD_3$, 121.5 MHz, 20°C): δ = 76.65 (br, 2P); ^{13}C NMR ($C_6D_5CD_3$, 125 MHz, 20°C): δ = 211.2 (Mn–C), 110.8 (C–Si), 34.7 (m, 2C; PCH$_2$), 30.2 (m, 2C; PCH$_2$), 22.9 (m, 2C; PCH$_3$), 20.9 (m, 2C; PCH$_3$), 20.5 (m, 2C; PCH$_3$), 14.5 (m, 2C; PCH$_3$), 8.5 (s, 6C; SiCH$_2$CH$_3$), 6.5 (s, 6C; SiCH$_2$C*H*$_3$); ^{29}Si NMR ($C_6D_5CD_3$, 99.38 MHz, 20°C): δ = −26.6 (t); IR (CH_2Cl_2, 20°C): $\tilde{\nu}$ = 1987 (ν(C≡C)), 1944 cm^{-1} (ν(C≡C)); elemental analysis calcd (%) for $C_{28}H_{62}MnNaP_4Si_2$ (656.8): C 51.20, H 9.51; found: C 51.40, H 9.52.

Synthesis of [Mn(dmpe)$_2$(C≡CSiEt$_3$)(=C=C(H)(SiEt$_3$))] (4b): MeOH (0.019 mL) was added to a solution of **3b** (0.60 mmol) in toluene (15 mL). The mixture was stirred for 1.5 h at room temperature to yield a yellow solution. The solvent was removed in vacuo, the product was extracted with pentane, and concentration of the extracts gave yellow crystals of **3b** (330 mg, 90%). ^{1}H NMR (C_6D_6, 300 MHz, 20°C): δ = 3.05 (quint, J_{PH} = 11.7 Hz, 1H; =CH), 1.50 (br, 4H; PCH$_2$), 1.43 (s, 12H; PCH$_3$), 1.36 (s, 12H; PCH$_3$), 1.30 (s, 4H; PCH$_2$), 1.17 (t, 9H; SiCH$_2$C*H*$_3$), 1.09 (t, 9H; SiCH$_2$C*H*$_3$), 0.63 (q, 6H; SiC*H*$_2$CH$_3$), 0.48 (q, 6H; SiC*H*$_2$CH$_3$); ^{31}P NMR (C_6D_6, 121.5 MHz, 20°C): δ = 68.49; ^{13}C NMR (C_6D_6, 125 MHz, 20°C): δ = 335.5 (quint, $^2J_{PC}$ = 25 Hz; Mn=C), 170.2 (quint, $^2J_{PC}$ = 27 Hz; Mn–C), 125.8 (C–Si), 88.5 (=CH), 31.8 (m, PCH$_2$), 17.9 (m, PCH$_3$), 8.9 (CH$_2$*C*H$_3$Si), 8.5 (CH$_2$*C*H$_3$Si), 6.7 (*C*H$_2$CH$_3$Si), 6.5 (*C*H$_2$CH$_3$Si); IR (CH_2Cl_2, 20°C): $\tilde{\nu}$ = 1988 (ν(C≡C)), 1947 (ν(C=C)), 1598 (ν(C≡C)), 1550 cm^{-1} (ν(C=C)); elemental analysis calcd (%) for $C_{28}H_{63}MnP_4Si_2$ (634.8): C 52.97, H 10.00; found: C 52.72, H 9.91.

Synthesis of [Mn(dmpe)$_2$(C≡CSiEt$_3$)(=C=CH$_2$)] (5b): A solution of KOH in MeOH (1 mL) was added to a solution of **4b** (0.52 mmol) in toluene (15 mL). The mixture was stirred for 1 h at room temperature, during which it turned light yellow. The solvent was removed in vacuo, the product was extracted with pentane, and concentration of the extracts gave light-green crystals of **5b** (220 mg, 80%). ^{1}H NMR (C_6D_6, 300 MHz, 20°C): δ = 3.55 (q, $^4J_{PH}$ = 11.5 Hz), 1.48 (br, 4H; PCH$_2$), 1.42 (s, 12H; PCH$_3$), 1.34 (s, 12H; PCH$_3$), 1.28 (s, 4H; PCH$_2$), 1.17 (t, 18H; SiCH$_2$C*H*$_3$), 0.71 (q, 12H; SiC*H*$_2$CH$_3$); ^{31}P NMR (C_6D_6, 121.5 MHz, 20°C): δ = 68.96; ^{13}C NMR (C_6D_6, 125 MHz, 20°C): δ = 343.5 (quint, $^2J_{PC}$ = 28.5 Hz; Mn=C), 169.8 (quint, $^2J_{PC}$ = 26 Hz; Mn–C), 124.4 (C–Si), 89.5 (quint, $^3J_{PC}$ = 4.1 Hz; =CH$_2$), 31.8 (m, PCH$_2$), 17.9 (m, PCH$_3$), 8.9 (CH$_2$*C*H$_3$Si), 6.5 (*C*H$_2$CH$_3$Si); ^{29}Si NMR (C_6D_6, 99.38 MHz, 20°C): δ = −21.2 (q, $^4J_{PSi}$ = 2.5 Hz); IR (CH_2Cl_2, 20°C): $\tilde{\nu}$ = 1988 (ν(C≡C)), 1945 (ν(C≡C)), 1595 (ν(C=C)), 1542 cm^{-1} (ν(C=C)); elemental analysis calcd (%) for $C_{22}H_{49}MnP_4Si$ (520.5): C 50.76, H 9.48; found: C 50.49, H 9.26.

Synthesis of [Mn(dmpe)$_2$(C≡CSiMe$_3$)(C≡CH)][PF$_6$] (7a): Quinuclidine (0.25 mmol) was added to a solution of [Mn(dmpe)$_2$(C≡CSiMe$_3$)(C=CH$_2$)] (100 mg, 0.21 mmol) in THF, and after stirring for 5 min [Cp$_2$Fe][PF$_6$] (140 mg, 0.42 mmol) was added. The dark-red solution formed was stirred at room temperature. After 1 h, the solvent was removed in vacuo and the residue was washed with Et_2O to yield a red solid. This was finally extracted with CH_2Cl_2 yielding pure **7a** (110 mg, 75%). ^{1}H NMR (CD_2Cl_2, 300 MHz, 20°C): δ = 7.87 (br, 9H; SiMe$_3$), −29.40 (br, 8H; PCH$_2$), −38.80 (br, 12H; PCH$_3$), −39.80 (br, 12H; PCH$_3$), (C≡CH) not observed; ^{31}P NMR (CD_2Cl_2, 121.5 MHz, 20°C): δ = −145.5 (sept, J = 718 Hz, 1P; PF$_6$); ^{19}F NMR (CD_2Cl_2, 20°C, 282.32 MHz): δ = −75.4 (d, J = 718 Hz, 6F; PF$_6$); IR (CH_2Cl_2, 20°C): $\tilde{\nu}$ = 2020, 1919 cm^{-1} (ν(C≡C)); elemental analysis calcd (%) for $C_{19}H_{42}P_5F_6MnSi$ (622.4): C 36.66, H 6.80; found: C 36.94, H 6.99.

Reaction of complex 7a with Cp$_2$Co: Cp$_2$Co (31 mg, 0.16 mmol) was added to a solution of **7a** (100 mg, 0.16 mmol) in THF. The mixture was stirred for 2 h and then concentrated to dryness. The residue was extracted with pentane (3×5 mL), and the combined extracts were filtered through Celite and concentrated to give 30 mg of a yellow solid. This solid had previously been characterized as a mixture of the complex [Mn(dmpe)$_2$(C≡CSiMe$_3$)(C≡CH)] (**8a**) and the [Mn(dmpe)$_2$(C≡CSiMe$_3$)(C=CH$_2$)] species.[51] ^{1}H NMR data for **8a** (C_6D_6, 300 MHz, 20°C): δ = 4.86 (br, 9H; SiMe$_3$), −13.20 to −16.40 (br, 32H; dmpe), (C≡CH not observed); elemental analysis calcd (%) for $C_{19}H_{42}P_4MnSi$ (477.4): C 47.80, H 8.87 and for $C_{19}H_{41}P_4MnSi$ (476.4): C 47.90, H 8.67; found for the mixture: C 47.66, H 8.95.

Synthesis of [Mn(dmpe)$_2$(C≡CSiEt$_3$)(C≡CH)][PF$_6$] (7b): Quinuclidine (0.23 mmol) was added to a solution of [Mn(dmpe)$_2$(C≡CSiEt$_3$)(C=CH$_2$)] (100 mg, 0.19 mmol) in THF, and after stirring for 5 min [Cp$_2$Fe][PF$_6$] (140 mg, 0.38 mmol) was added. The dark-red solution formed was stirred at room temperature. After 1 h, the solvent was removed in vacuo and the residue was washed with Et_2O to yield a red solid. This was extracted with CH_2Cl_2 yielding pure **7b**. The compound was crystallized from THF (100 mg, 79%). ^{1}H NMR (CD_2Cl_2, 300 MHz, 20°C): δ = 6.69 (br, 1H; C≡CH) 3.37 (br, 9H; SiCH$_2$C*H*$_3$), 1.93 (br, 6H; SiC*H*$_2$CH$_3$), −29.53 (br, 8H; PCH$_2$), −39.34 (br, 12H; PCH$_3$), −39.80 (br, 12H; PCH$_3$); ^{31}P NMR (CD_2Cl_2, 121.5 MHz, 20°C): δ = −145.5 (sept, J = 718 Hz, 1P; PF$_6$); ^{19}F NMR (CD_2Cl_2, 282.32 MHz, 20°C): δ = −75.4 (d, J = 718 Hz, 6F; PF$_6$); IR (CH_2Cl_2, 20°C): $\tilde{\nu}$ = 2020, 1919 cm^{-1} (ν(C≡C)); elemental analysis calcd (%) for $C_{22}H_{48}P_5F_6MnSi$ (664.34): C 39.76, H 7.28; found: C 39.56, H 7.18.

Synthesis of [Mn(dmpe)$_2$(C≡CSiEt$_3$)(C≡CH)] (8b): Cp$_2$Co (31 mg, 0.15 mmol) was added to a solution of **7b** (100 mg, 0.15 mmol) in CH_2Cl_2 (10 mL). The mixture was stirred for 2 h and then concentrated to dryness. The residue was extracted with pentane (3×5 mL), and the combined extracts were filtered through Celite and concentrated to give yellow **8b** (40 mg, 51%). ^{1}H NMR data for **8b** (C_6D_6, 300 MHz, 20°C): δ = 6.69 (br, 1H; C≡CH), 1.30 (br, 9H; SiCH$_2$C*H*$_3$), 0.84 (br, 6H; SiC*H*$_2$CH$_3$), −14.27 (br, 8H; PCH$_2$), −15.07 (br, 12H; PCH$_3$), −15.74 (br, 12H; PCH$_3$); IR (CH_2Cl_2, 20°C): $\tilde{\nu}$ = 2015, 1916 cm^{-1} (ν(C≡C)); elemental analysis calcd (%) for $C_{22}H_{48}P_4MnSi$ (519.53): C 50.86, H 9.31; found: C 50.56, H 9.22.

Synthesis of [Mn(dmpe)$_2$(C≡CSiMe$_3$)I] (9): A solution of Me$_3$SnC≡CSiMe$_3$ (80 mg, 0.30 mmol) in THF (2 mL) was added to a suspension of Mn(MeCp)(dmpe)I (100 mg, 0.24 mmol) in the same solvent. An orange solution was formed within 10 min of stirring, and then dmpe (38 mg, 0.25 mmol) was added. After 1 h, the solvent was removed in vacuo and the residue was extracted with hexane. The dark-red solution was concentrated and chilled to −30°C to yield red crystals of **6** (60 mg, 40%). ^{1}H NMR (C_6D_6, 300 MHz, 20°C): δ = 6.08 (br, 9H; SiMe$_3$), −13.5 (br, 8H; PCH$_2$), −17.6 (br, 24H; PCH$_3$); IR (C_6H_6, 20°C): $\tilde{\nu}$ = 1954, 1807 cm^{-1} (ν(C≡C)); elemental analysis calcd (%) for $C_{17}H_{41}IMnP_4Si$ (579.33): C 35.24, H 7.13; found: C 35.49, H 7.21. Single crystals of **6** were obtained from a saturated solution in pentane at −30°C.

Reaction of [Mn(dmpe)$_2$(C≡CSiR$_3$)$_2$]PF$_6$ complexes with TBAF—Synthesis of [{Mn(dmpe)$_2$(C≡CH)}$_2$(μ-C$_4$)][PF$_6$] ([11]$^+$): TBAF (0.18 mL of a 1.0 M solution in THF) was added to a solution of species **2** (0.18 mmol) in CH_2Cl_2 (5 mL). The reaction mixture was stirred for 2 h at room tem-

perature (20°C) and then the solvent was removed in vacuo. The dark solid was extracted with hexane to give a yellow solution, which still contained traces of the dinuclear species **11** together with traces of other unidentified complexes. After removal of the solvent, the dark residue was washed with THF and finally extracted with CH_2Cl_2 to give **[11]$^+$** as a violet solid. Yield starting from: **2a** (110 mg, 65%), **2b** (110 mg, 65%), **2c** (63 mg, 37%). ^{1}H NMR (CD_2Cl_2, 300 MHz, 20°C): δ = −0.29 (br, 8H; PCH_2), −4.60 (br, 24H; PCH_3), −6.55 (br, 24H; PCH_2), −6.71 (br, 24H; PCH_3), −46.39 (br, 2H; ≡CH); ^{31}P NMR (CD_2Cl_2, 121.47 MHz, 20°C, 85% H_3PO_4 ext.): δ = −145.62 (sept, $^1J_{PF}$ = 717.9 Hz; PF_6^-); ^{19}F NMR (CD_2Cl_2, 282.32 MHz, 20°C, $C_6H_5CF_3$ ext.): δ = −75.09 (d, J = 717.9 Hz; PF_6^-); IR (CH_2Cl_2, 20°C): $\tilde{\nu}$ = 2140 (s), 1819 (w) (νC_4); 1960 cm^{-1} (w) (ν(C≡CH)); elemental analysis calcd (%) for $C_{32}H_{66}F_6Mn_2P_9$ (953.49): C 40.31, H 6.98; found: C 40.01, H 6.80.

Synthesis of [{Mn(dmpe)$_2$(C≡CSiMe$_3$)}$_2$(μ-C$_4$)][PF$_6$] ([12]$^+$): DBU (0.040 mL, 0.22 mmol) was added to a solution of species **7a** (140 mg, 0.23 mmol) in THF (10 mL). A fast colour change from red to dark-green was observed. The solution was stirred for 1.5 h. The solvent was then removed in vacuo and the residue was washed with hexane. Recrystallization from THF/Et_2O yielded violet crystals of **[12]$^+$** (150 mg, 60%). ^{1}H NMR (CD_2Cl_2, 300 MHz, 20°C,): δ = 0.72 (s, 18H; $SiMe_3$), −0.26 (br, 8H; PCH_2), −4.57 (br, 24H; PCH_3), −6.40 (br, 8H; PCH_2), −6.69 (br, 24H; PCH_3); ^{31}P NMR (CD_2Cl_2, 121.47 MHz, 20°C, 85% H_3PO_4 ext.): δ = −145.12 (sept, $^1J_{PF}$ = 717.9 Hz; PF_6^-); ^{19}F NMR (CD_2Cl_2, 282.32 MHz, 20°C, $C_6H_5CF_3$ ext.): δ = −74.72 (d, J = 717.9 Hz; PF_6^-); IR (CH_2Cl_2, 20°C): $\tilde{\nu}$ = 1990 (ν(C≡C)); 2016 (w), 1879 cm^{-1} (w) ($\nu(C_4)$); elemental analysis calcd (%) for $C_{38}H_{82}F_6Mn_2P_9Si_2$ (1097.8): C 41.57, H 7.52; found: C 41.40, H 7.80. Violet single crystals of **[12]$^+$** were obtained from solutions in THF/Et_2O (1:1) at −30°C.

Synthesis of [{Mn(dmpe)$_2$(C≡CH)}$_2$(μ-C$_4$)] (11): Cp(C_6Me_6)Fe (15 mg, 0.052 mmol) was added to a suspension of **[11]$^+$** (50 mg, 0.052 mmol) in THF. The mixture was stirred for 2 h and then the solvent was removed in vacuo. The product was extracted with pentane to give **11** as a dark-green solid (38 mg, 90%). ^{1}H NMR (C_6D_6, 300 MHz, 40°C): δ = −9.47 (br, 8H; PCH_2), −14.9 (br, 32H; PMe_3 + PCH_2), −18.78 (br, 24H; PCH_3); −149.4 (br, 2H; ≡CH); IR: no ν(C≡C) are observed; elemental analysis calcd (%) for $C_{32}H_{66}Mn_2P_8$ (808.53): C 47.54, H 8.23; found: C 47.62, H 8.53.

Synthesis of [{Mn(dmpe)$_2$(C≡CSiMe$_3$)}$_2$(μ-C$_4$)] (12): Cp(C_6Me_6)Fe (23 mg, 0.09 mmol) was added to a solution of species **[12]$^+$** (100 mg, 0.09 mmol) in THF (10 mL). The mixture was stirred for 1 h and then the solvent was removed in vacuo. The product was extracted with pentane to yield **12** as a green solid (67 mg, 78%). ^{1}H NMR (C_6D_6, 300 MHz, 20°C): δ = 2.85 (s, 18H; $SiMe_3$), −10.42 (br, 8H; PCH_2), −15.83 (br, 8H; PCH_2), −16.43 (br, 24H; PCH_3), −20.35 (br, 24H; PCH_3); elemental analysis calcd (%) for $C_{38}H_{82}Mn_2P_8Si_2$ (952.9): C 47.89, H 8.67; found: C 47.70, H 8.66.

Reaction of [Mn(dmpe)$_2$(C≡CSiR$_3$)$_2$]$^+$ species with TBAF in the presence of TEMPO: TBAF (0.18 mL of a 1.0 M solution in THF) was added to a solution of **2** (0.18 mmol) and TEMPO (0.54 mmol) in CH_2Cl_2 (5 mL). The reaction mixture was stirred for 2 h at room temperature (20°C) and then the solvent was removed in vacuo. The dark solid was washed with cold hexane and extracted with toluene to give a yellow solution, which contained the Mn^I complex **14** (60%) and traces of other unidentified Mn^{II} compounds. The residue was washed with THF and finally extracted with CH_2Cl_2 to afford **7** as a violet solid (<15%). Data for **14**: ^{1}H NMR (C_6D_6, 300 MHz, 20°C): δ = 1.53, 1.45, 1.29, and 1.13 (s; PMe_3), 1.60 to 0.90 overlapping signals (br; PCH_2); ^{31}P NMR (C_6D_6, 121.47 MHz, 20°C, H_3PO_4 ext.): δ = 60.26 (s, 4P; dmpe). A few blue single crystals of **14** were obtained from hexane solutions of the reaction products.

Synthesis of [{Mn(dmpe)$_2$(C≡CH)}$_2$(μ-C$_4$)][PF$_6$]$_2$ ([11]$^{2+}$): [Cp_2Fe][PF_6] (17 mg, 0.052 mmol) was added to a solution of **[11]$^+$** (50 mg, 0.052 mmol) in CH_2Cl_2 (10 mL). The mixture was stirred for 3 h and then concentrated in vacuo to a volume of 2 mL. Addition of Et_2O caused the precipitation of **[11]$^{2+}$** as a brown solid (51 mg, 90%). ^{1}H NMR (CD_2Cl_2, 300 MHz, 20°C): δ = 1.93 (br, 8H; PCH_2), 1.83 (br, 24H; PCH_2), 1.38 (br, 24H; PCH_3), 1.27 (br, 24H; PCH_3), −2.30 (br, 2H; ≡CH); ^{31}P NMR (CD_2Cl_2, 121.47 MHz, 20°C, 85% H_3PO_4 ext.): δ = −145.44 (sept, $^1J_{PF}$ = 719 Hz; PF_6^-); ^{19}F NMR (CD_2Cl_2, 282.32 MHz, 20°C, $C_6H_5CF_3$ ext.): δ = −74.02 (d, J = 719 Hz; PF_6^-); IR (KBr, 20°C): $\tilde{\nu}$ = 1929 (ν(C≡C)); 2025, 1915, 1920 cm^{-1} ($\nu(C≡C)_2$); elemental analysis calcd (%) for $C_{32}H_{66}F_{12}Mn_2P_{10}$ (1098.46): C 34.99, H 6.06; found: C 34.86, H 6.06.

Synthesis of [{Mn(dmpe)$_2$(C≡CSiMe$_3$)}$_2$(μ-C$_4$)][PF$_6$]$_2$ ([12]$^{2+}$): [Cp_2Fe][PF_6] (30 mg, 0.09 mmol) was added to a solution of **[12]$^+$** (100 mg, 0.09 mmol) in CH_2Cl_2 (10 mL). An immediate colour change from dark-red to brown occurred. The mixture was stirred for 1 h and then concentrated in vacuo to a volume of 2 mL. The product was precipitated by the addition of Et_2O to yield **[12]$^{2+}$** as a red-brown solid (100 mg, 89%). ^{1}H NMR (CD_2Cl_2, 300 MHz, 20°C): δ = 1.92 (br, 16H; PCH_2), 1.40 (br, 24H; PCH_3), 1.32 (br, 24H; PCH_3), −0.14 (s, 18H; $SiMe_3$); ^{31}P NMR (CD_2Cl_2, 121.47 MHz, 20°C, 85% H_3PO_4 ext.): δ = −141.62 (sept, $^1J_{PF}$ = 720 Hz; PF_6^-); ^{19}F NMR (CD_2Cl_2, 282.32 MHz, 20°C, $C_6H_5CF_3$ ext.): δ = −73.30 (d, J = 720 Hz; PF_6^-); IR (CH_2Cl_2, 20°C): $\tilde{\nu}$ = 2010 (w), 1650 cm^{-1} (br); elemental analysis calcd (%) for $C_{38}H_{82}F_{12}Mn_2P_{10}Si_2$ (1242.8): C 36.72, H 6.65; found: C 36.53, H 6.63. Brown-orange single crystals of **[12]$^{2+}$** were obtained from saturated solutions in THF at −30°C.

Crystallographic studies of compounds 4b, 7b, 9, [12]$^+$, [12]$^{2+}$, and 14: The crystals were mounted on top of a glass fibre using polybutene oil as protecting agent. Crystals of compound **[12]$^+$** were extremely sensitive towards mechanical touch. Thus, the selected crystal was carefully included in a glass capillary of 0.3 mm diameter together with the protective oil. The crystals were cooled to 153(2) K (**4b**, **[12]$^+$**, **[12]$^{2+}$**, **14**) or 183(2) K (**7b**, **9**) by means of an Oxford cryogenic system. The determination of the unit cell parameters and the collection of intensity data were performed with an image plate detector system (STOE IPDS diffractometer) and graphite-monochromated $Mo_{K\alpha}$ radiation (λ = 0.71073 Å) using the STOE IPDS software, Version No. 2.92 (1999). A total of 200, 197, 200, 214, 167, and 230 images were exposed at constant times of 2.50, 4.00, 3.00, 9.00, 2.80, and 10.00 min per image for **4b**, **7b**, **9**, **[12]$^+$**, **[12]$^{2+}$**, and **14**, respectively. The total exposure and read-out times for the six compounds were 22, 28, 24, 47, 27, and 39 h in the order of the complexes as given above. The crystal-to-image distances were set to 50, 60, 60, 70, 54, and 50 mm (θ_{max} = 30.25, 27.97, 28.0, 26.21, 29.34, and 30.44°). ϕ oscillation scan modes (**4b**, **7b**, **9**, **[12]$^+$**, **[12]$^{2+}$**, and **14**) were selected for ϕ increments of 1.0, 1.2, 1.0, 1.4, 1.0, and 1.2° per exposure. A total of 8000 reflections (4993 for **[12]$^+$** and 7073 for **14**) with $I > 6\sigma(I)$ were selected from the whole limiting sphere for the cell parameter refinements. Lorentz and polarization corrections were applied with INTEGRATE and numerical absorption corrections[101] were applied with XRED using a video camera installed within the IPDS diffractometer. The structures were solved by direct methods and the Patterson method using SHELXS-97.[102] All refinements were performed with SHELXL-97.[103] ORTEP ellipsoid plots were generated with PLATON.[104] Summaries of crystal data and refinements are given in Tables 2 and 3. For compound **4b**, the anisotropic displacement parameters of atoms C1, C2 and C3, C4 became very large during the refinement. Furthermore, a distinction between the vinylidene and alkynyl moieties based on distance and angle criteria was not possible. Thus, the different ligands were refined with distance restraints (DFIX) and as split atoms using the EADP and PART instructions of SHELXL-97.[103]

A minor merohedric twinning effect was noticed during refinement of Flack's absolute structure parameter x[105] [x = 0.152(13)] for the non-centrosymmetric structure of **9**. The twin ratio is hence about 85:15. Some practical aspects on "*Reporting and evaluating absolute structure and absolute configuration determination*" are given by Flack and Bernardinelli.[106]

With respect to the relatively high R values of compound **[12]$^+$**, it should be noted that only 37.8% of the unique data are observed. This may result from additional background intensity of the glass capillary and the protective oil. Furthermore, none of the monoclinic standard space groups ($C2$, Cc, Cm, $C2m^{-1}$, $C2/c$) gave any model that could be refined successfully. The structure was finally solved and refined in the centrosymmetric space group $C2/m$, and no disorder was observed. These findings may be due to an unresolved twinning problem that was probably generated during the difficult sample preparation.

For compound **[12]$^{2+}$**, high displacement parameter values and a poor geometry of the THF solvent molecule were noticed. Attempts to optimize the THF geometry by using restraints (DFIX) failed, probably due

Table 2. Crystallographic data and structure refinement for compounds **4b**, **7b**, **9**, and **[12]$^+$**.

	4b	**7b**	**9**	**[12]$^+$**
formula	$C_{28}H_{63}MnP_4Si_2$	$C_{22}H_{48}F_6MnP_5Si$	$C_{17}H_{41}IMnP_4Si$	$C_{38}H_{82}F_6Mn_2P_9Si_2$
color	yellow	yellow	dark-red	violet
crystal dimensions [mm]	$0.27\times0.25\times0.21$	$0.23\times0.21\times0.03$	$0.25\times0.12\times0.10$	$0.33\times0.16\times0.01$
crystal system	monoclinic	monoclinic	orthorhombic	monoclinic
space group (no.)	$P2_1/c$ (14)	$C2/c$ (15)	$P2_12_12_1$ (19)	$C\bar{1}$[a]
a [Å]	15.7638(13)	9.2228(7)	9.4269(5)	11.2167(12)
b [Å]	11.3919(7)	31.154(2)	16.5675(9)	16.6768(18)
c [Å]	20.7090(17)	11.6293(8)	17.3037(9)	15.3388(16)
α,β,γ [°]	90, 104.95(9), 90	90, 90.970(8), 90	90, 90, 90	90, 91.028(13), 90
V [Å^3]	3607.0(5)	3343.5(4)	2702.5(2)	2868.8(5)
Z	4	4	4	2
M_r	634.78	664.48	579.31	1097.83
ρ_{calcd} [g cm^{-3}]	1.169	1.320	1.424	1.271
μ [mm^{-1}]	0.626	0.714	1.912	0.777
$F(000)$	1376	1392	1180	1154
2θ scan range [°]	$5.40<2\theta<60.54$	$4.38<2\theta<55.94$	$5.50<2\theta<56.00$	$5.08<2\theta<52.42$
no. measured, unique data	41449, 10389 (R_{int} = 0.0972)	14379, 3855 (R_{int} = 0.1018)	25929, 6451 (R_{int} = 0.0432)	16873, 5228 (R_{int} = 0.2068)
no. data obsd. [$I>2\sigma(I)$]	5120	2191	5547	1978
absorption correction	numerical, 15 crystal faces	numerical, 6 crystal faces	numerical, 14 crystal faces	numerical, 8 crystal faces
transmission range	0.8798–0.8493	0.9789–0.8529	0.8318–0.6464	0.9915–0.7835
no. parameters refined	323	169	214	268
$R1$, $wR2$ [%] all data	7.84, 9.52	13.94, 10.41	3.02, 4.97	16.92, 22.46
$R1$ (obsd.) [%][b]	4.34	5.38	2.39	8.85
GoF	1.021	0.882	0.890	0.997

[a] See Experimental Section. [b] $R1 = \Sigma(F_o-F_c)/\Sigma F_o$; $I>2\sigma(I)$; $wR2 = \{\Sigma w(F_o^2-F_c^2)^2/\Sigma w(F_o^2)^2\}^{1/2}$.

to the weak diffraction power of the crystal. About 50% of the reflection data are unobserved by the criterion $I<2\sigma(I)$. The THF molecule was finally refined with isotropic displacement parameters.

Table 3. Crystallographic data and structure refinement for compounds **14** and **[12]$^{2+}$**.

	14	**[12]$^{2+}$**
formula	$C_{23}H_{41}MnO_2P_4$	$C_{42}H_{90}F_{12}Mn_2OP_{10}Si_2$
color	blue	brown
crystal dimensions [mm]	$0.25\times0.12\times0.03$	$0.47\times0.26\times0.04$
crystal systems	monoclinic	triclinic
space group (no.)	$P2/c$ (13)	$P\bar{1}$ (2)
a [Å]	9.3543(5)	10.0201(6)
b [Å]	12.5147(8)	16.6766(10)
c [Å]	11.5234(7)	19.6488(13)
α, β, γ [°]	90, 96.530(7), 90	86.644(7), 88.043(8), 81.011(7)
V [Å^3]	1340.25(14)	3236.4(3)
Z	2	2
M_r	528.38	1314.90
ρ_{calcd} [g cm^{-3}]	1.309	1.349
μ [mm^{-1}]	0.748	0.738
$F(000)$	560	1372
2θ scan range [°]	$6.24<2\theta<60.88$	$4.82<2\theta<58.68$
no. measured, unique data	13976, 3733 (R_{int} = 0.0878)	40866, 16247(R_{int} = 0.0743)
no. data obsd. [$I>2\sigma(I)$]	2094	8085
absorption correction	numerical, 6 crystal faces	numerical, 8 crystal faces
transmission range	0.9764–0.8344	0.9711–0.7229
no. parameters refined	143	619
$R1$, $wR2$ [%] all data	8.58, 9.23	10.59, 10.96
$R1$ (obsd.) (%)[a]	3.96	4.74
goodness-of-fit	0.830	1.008

[a] $R1 = \Sigma(F_o-F_c)/\Sigma F_o$; $I>2\sigma(I)$; $wR2 = \{\Sigma w(F_o^2-F_c^2)^2/\Sigma w(F_o^2)^2\}^{1/2}$.

Computational details: DFT calculations were carried out using the Amsterdam Density Functional program package ADF, release 2002.02.[107] We used the Vosko–Wilk–Nusair[108] local density approximation (LDA) and the generalized gradient approximation (GGA) with corrections for exchange and correlation according to Becke[109] and Perdew,[110] respectively (BP86). The ADF approach to DFT GGA calculations is based on the use of Slater-type orbitals (STO) as basis functions. The valence shells of all non-hydrogen atoms were described by triple-ξ basis sets augmented by one polarization function (ADF database TZP), while a standard double-ξ basis set was applied for hydrogen atoms (ADF database DZP). The frozen-core approximation was applied for the 1s electrons of carbon atoms, for the 1s–2p electrons of phosphorus, silicon, and manganese, and for the 1s–4p electrons of iodine atoms. The geometry optimizations were considered converged when the change in total energy was less than 10^{-4} Hartrees and the maximum gradient element was smaller than 2.5×10^{-3} Hartrees Å^{-1}. The other convergence criteria referring to changes in the Cartesian or internal coordinates had to converge to the default values proposed by the program. The numerical integration precision parameter, based on a method developed by te-Velde,[111] was chosen in such a way that significant test integrals were evaluated with an accuracy of at least four significant decimal digits. For systems with an odd electron count, spin-unrestricted calculations were performed. The solvation energies based on gas-phase geometries were calculated by means of the conductor-like screening model (COSMO) suggested by Klamt and Schuurmann[112] and implemented in ADF by Pye and Ziegler.[113] The solvent-accessible surface was chosen and constructed using the following radii: H 1.16, C 2.00, P 1.70, Si 2.20, I 2.30, and Mn 2.40 Å. A dielectric constant of 7.58 was used for THF.

CCDC-190113 (**4b**), -190114 (**7b**), -190115 (**9**), -190116 (**[12]$^+$**), -190117 (**14**), and -190118 (**[12]$^{2+}$**) contain the supplementary crystallographic data for this paper. These data can be obtained free of charge via www.ccdc.cam.ac.uk/conts/retrieving.html, or from the Cambridge Crystallographic Data Centre, 12 Union Road, Cambridge CB2 1EZ, UK; fax: (+44)1223–336033; or email: deposit@ccdc.cam.ac.uk.

Acknowledgement

Funding from the Swiss National Science Foundation (SNSF) and from the University of Zürich is gratefully acknowledged.

[1] K. Sonogashira, T. Yatake, Y. Tohda, S. Takahashi, N. Hagihara, *Chem. Commun.* **1977**, 291.
[2] K. Sonogashira, S. Takahashi, N. Hagihara, *Macromolecules* **1977**, *10*, 879.
[3] K. Sonogashira, Y. Fujikura, T. Yatake, N. Toyoshima, S. Takahashi, N. Hagihara, *J. Organomet. Chem.* **1978**, *145*, 101.
[4] Y. Sun, N. J. Taylor, A. J. Carty, *Organometallics* **1992**, *11*, 4293.
[5] R. D. Markwell, I. S. Butler, A. K. Kakkar, M. S. Khan, Z. H. Al-Zakwani, J. Lewis, *Organometallics* **1996**, *15*, 2331.
[6] F. Paul, C. Lapinte, *Coord. Chem. Rev.* **1998**, *180*, 431.
[7] F. Paul, K. Costuas, I. Ledoux, S. Deveau, J. Zyss, J. F. Halet, C. Lapinte, *Organometallics* **2002**, *21*, 5229.
[8] F. Paul, J. Y. Mevellec, C. Lapinte, *J. Chem. Soc. Dalton Trans.* **2002**, 1783.
[9] S. K. Hurst, M. P. Cifuentes, A. M. McDonagh, M. G. Humphrey, M. Samoc, B. Luther-Davies, I. Asselberghs, A. Persoons, *J. Organomet. Chem.* **2002**, *642*, 259.
[10] R. D'Amato, A. Furlani, M. Colapietro, G. Portalone, M. Casalboni, M. Falconieri, M. V. Russo, *J. Organomet. Chem.* **2001**, *627*, 13.
[11] R. Denis, L. Toupet, F. Paul, C. Lapinte, *Organometallics* **2000**, *19*, 4240.
[12] J. Gil-Rubio, M. Laubender, H. Werner, *Organometallics* **2000**, *19*, 1365.
[13] V. Grosshenny, A. Harriman, R. Ziessel, *Angew. Chem.* **1995**, *107*, 2921; *Angew. Chem. Int. Ed. Engl.* **1995**, *34*, 2705.
[14] E. Hendrickx, A. Persoons, S. Samson, G. R. Stephenson, *J. Organomet. Chem.* **1997**, *542*, 295.
[15] J. H. K. Yip, J. G. Wu, K. Y. Wong, K. W. Yeung, J. J. Vittal, *Organometallics* **2002**, *21*, 1612.
[16] J. M. Tour, *Acc. Chem. Res.* **2000**, *33*, 791.
[17] K. T. Wong, J. M. Lehn, S. M. Peng, G. H. Lee, *Chem. Commun.* **2000**, 2259.
[18] C. P. Collier, J. O. Jeppesen, Y. Luo, J. Perkins, E. W. Wong, J. R. Heath, J. F. Stoddart, *J. Am. Chem. Soc.* **2001**, *123*, 12632.
[19] J. M. Tour, A. M. Rawlett, M. Kozaki, Y. X. Yao, R. C. Jagessar, S. M. Dirk, D. W. Price, M. A. Reed, C. W. Zhou, J. Chen, W. Y. Wang, I. Campbell, *Chem. Eur. J.* **2001**, *7*, 5118.
[20] M. Shiotsuka, Y. Yamamoto, S. Okuno, M. Kitou, K. Nozaki, S. Onaka, *Chem. Commun.* **2002**, 590.
[21] S. Le Stang, F. Paul, C. Lapinte, *Organometallics* **2000**, *19*, 1035.
[22] M. I. Bruce, B. D. Kelly, B. W. Skelton, A. H. White, *J. Organomet. Chem.* **2000**, *604*, 150.
[23] J. M. Tour, M. Kozaki, J. M. Seminario, *J. Am. Chem. Soc.* **1998**, *120*, 8486.
[24] L. A. Bumm, J. J. Arnold, M. T. Cygan, T. D. Dunbar, T. P. Burgin, L. Jones, D. L. Allara, J. M. Tour, P. S. Weiss, *Science* **1996**, *271*, 1705.
[25] A. Harriman, R. Ziessel, *Chem. Commun.* **1996**, 1707.
[26] J. M. Tour, *Chem. Rev.* **1996**, *96*, 537.
[27] M. A. Reed, C. Zhou, C. J. Muller, T. P. Burgin, J. M. Tour, *Science* **1997**, *278*, 252.
[28] D. L. Pearson, L. Jones, J. S. Schumm, J. M. Tour, *Synth. Met.* **1997**, *84*, 303.
[29] A. Harriman, R. Ziessel, *Coord. Chem. Rev.* **1998**, *171*, 331.
[30] C. P. Collier, E. W. Wong, M. Belohradsky, F. M. Raymo, J. F. Stoddart, P. J. Kuekes, R. S. Williams, J. R. Heath, *Science* **1999**, *285*, 391.
[31] A. R. Pease, J. O. Jeppesen, J. F. Stoddart, Y. Luo, C. P. Collier, J. R. Heath, *Acc. Chem. Res.* **2001**, *34*, 433.
[32] F. Paul, W. E. Meyer, L. Toupet, H. J. Jiao, J. A. Gladysz, C. Lapinte, *J. Am. Chem. Soc.* **2000**, *122*, 9405.
[33] M. I. Bruce, P. J. Low, K. Costuas, J. F. Halet, S. P. Best, G. A. Heath, *J. Am. Chem. Soc.* **2000**, *122*, 1949.
[34] W. Q. Weng, T. Bartik, M. Brady, B. Bartik, J. A. Ramsden, A. M. Arif, J. A. Gladysz, *J. Am. Chem. Soc.* **1995**, *117*, 11922.
[35] T. Ren, G. Zou, J. C. Alvarez, *Chem. Commun.* **2000**, 1197.
[36] M. Brady, W. Q. Weng, Y. L. Zhou, J. W. Seyler, A. J. Amoroso, A. M. Arif, M. Bohme, G. Frenking, J. A. Gladysz, *J. Am. Chem. Soc.* **1997**, *119*, 775.
[37] T. Rappert, O. Nurnberg, H. Werner, *Organometallics* **1993**, *12*, 1359.
[38] V. W. W. Yam, V. C. Y. Lau, K. K. Cheung, *Organometallics* **1996**, *15*, 1740.
[39] M. Akita, M. C. Chung, A. Sakurai, S. Sugimoto, M. Terada, M. Tanaka, Y. Morooka, *Organometallics* **1997**, *16*, 4882.
[40] F. Coat, M. A. Guillevic, L. Toupet, F. Paul, C. Lapinte, *Organometallics* **1997**, *16*, 5988.
[41] M. Guillemot, L. Toupet, C. Lapinte, *Organometallics* **1998**, *17*, 1928.
[42] J. S. Schumm, D. L. Pearson, L. Jones, R. Hara, J. M. Tour, *Nanotechnology* **1996**, *7*, 430.
[43] R. L. Carroll, C. B. Gorman, *Angew. Chem.* **2002**, *114*, 455; *Angew. Chem. Int. Ed.* **2002**, *41*, 4378.
[44] M. J. Crossley, L. A. Johnston, *Chem. Commun.* **2002**, 1122.
[45] T. Otsuba, Y. Aso, K. Takimiya, *J. Mater. Chem.* **2002**, *12*, 2565.
[46] K. Sendt, L. A. Johnston, W. A. Hough, M. J. Crossley, N. S. Hush, J. R. Reimers, *J. Am. Chem. Soc.* **2002**, *124*, 9299.
[47] D. Unseld, Ph.D. Thesis, University of Zürich (Switzerland), **1999**.
[48] D. Unseld, V. V. Krivykh, K. Heinze, F. Wild, G. Artus, H. Schmalle, H. Berke, *Organometallics* **1999**, *18*, 1525.
[49] S. Kheradmandan, Ph.D. Thesis, University of Zürich (Switzerland), **2001**.
[50] S. Kheradmandan, K. Heinze, H. W. Schmalle, H. Berke, *Angew. Chem.* **1999**, *111*, 2412; *Angew. Chem. Int. Ed.* **1999**, *38*, 2270.
[51] F. J. Fernandez, M. Alfonso, H. W. Schmalle, H. Berke, *Organometallics* **2001**, *20*, 3122.
[52] F. J. Fernandez, O. Blacque, M. Alfonso, H. Berke, *Chem. Commun.* **2001**, 1266.
[53] V. V. Krivykh, I. L. Eremenko, D. Veghini, I. A. Petrunenko, D. L. Pountney, D. Unseld, H. Berke, *J. Organomet. Chem.* **1996**, *511*, 111.
[54] G. Eglinton, W. McCrae, *J. Chem. Soc.* **1963**, 2295.
[55] G. Albertin, S. Antoniutti, E. Bordignon, E. Delministro, S. Ianelli, G. Pelizzi, *J. Chem. Soc. Dalton Trans.* **1995**, 1783.
[56] V. Cadierno, S. Conejero, M. P. Gamasa, J. Gimeno, I. Asselberghs, S. Houbrechts, K. Clays, A. Persoons, J. Borge, S. Garcia-Granda, *Organometallics* **1999**, *18*, 582.
[57] B. Buriez, I. D. Burns, A. F. Hill, A. J. P. White, D. J. Williams, J. D. E. T. Wilton-Ely, *Organometallics* **1999**, *18*, 1504.
[58] M. P. Gamasa, J. Gimeno, M. Gonzalez-Cueva, E. Lastra, *J. Chem. Soc. Dalton Trans.* **1996**, 2547.
[59] R. L. Beddoes, C. Bitcon, R. W. Grime, A. Ricalton, M. W. Whiteley, *J. Chem. Soc. Dalton Trans.* **1995**, 2873.
[60] F. H. Köhler, N. Hebendanz, G. Muller, U. Thewalt, B. Kanellakopulos, R. Klenze, *Organometallics* **1987**, *6*, 115.
[61] G. S. Girolami, G. Wilkinson, A. M. R. Galas, M. Thorntonpett, M. B. Hursthouse, *J. Chem. Soc. Dalton Trans.* **1985**, 1339.
[62] ^{1}H NMR data for $[Mn(dmpe)_2(C{\equiv}CSiMe_3)I][PF_6]$ collected in CD_2Cl_2 at 20 °C: δ = 5.88 (s, 9H; $SiMe_3$), −30.98 (br, 4H; PCH_2), −33–36 (br, 4H; PCH_2), −41.10 (br, 12H; PCH_3), −41.92 (br, 12H; PCH_3).
[63] N. Lenarvor, L. Toupet, C. Lapinte, *J. Am. Chem. Soc.* **1995**, *117*, 7129.
[64] R. Dembinski, T. Lis, S. Szafert, C. L. Mayne, T. Bartik, J. A. Gladysz, *J. Organomet. Chem.* **1999**, *578*, 229.
[65] C. Chatgilialoglu, A. Guerrini, M. Lucarini, G. F. Pedulli, P. Carrozza, G. Da Roit, V. Borzatta, V. Lucchini, *Organometallics* **1998**, *17*, 2169.
[66] M. R. Terry, C. Kelley, N. Lugan, G. L. Geoffroy, B. S. Haggerty, A. L. Rheingold, *Organometallics* **1993**, *12*, 3607.
[67] U. Cremer, W. Kockelmann, M. Bertmer, U. Ruschewitz, *Solid State Sci.* **2002**, *4*, 247.
[68] R. Dembinski, T. Bartik, B. Bartik, M. Jaeger, J. A. Gladysz, *J. Am. Chem. Soc.* **2000**, *122*, 810.
[69] S. Hemmersbach, B. Zibrowius, W. Kockelmann, U. Ruschewitz, *Chem. Eur. J.* **2001**, *7*, 1952.
[70] K. M. C. Wong, C. K. Hui, K. L. Yu, V. W. W. Yam, *Coord. Chem. Rev.* **2002**, *229*, 123.
[71] M. Bigorgne, A. Loutelli, M. Pankowski, *J. Organomet. Chem.* **1970**, *23*, 201.
[72] J. G. Verkade, *Coord. Chem. Rev.* **1972**, *9*, 1.
[73] a) C. Creutz, *Prog. Inorg. Chem.* **1983**, *30*, 1; b) E. Heilbronner, H. Bock, *Das HMO-Modell und seine Anwendungen, Grundlagen und*

Handhabung, Verlag Chemie, Weinheim, Germany, **1968**, Chapter 12.2.
[74] P. Belanzoni, N. Re, A. Sgamellotti, C. Floriani, *J. Chem. Soc. Dalton Trans.* **1998**, 1825.
[75] J. C. Röder, F. Meyer, E. Kaifer, *Angew. Chem.* **2002**, *114*, 2414; *Angew. Chem. Int. Ed.* **2002**, *41*, 2304.
[76] D. Gudat, B. Lewall, M. Nieger, I. Detmer, L. Szarvas, P. Saarenketo, G. Marconi, *Chem. Eur. J.* **2003**, *9*, 661.
[77] Z. Y. Zhang, C. Broucacabarrecq, C. Hemmert, F. Dahan, J. P. Tuchagues, *J. Chem. Soc. Dalton Trans.* **1995**, 1453.
[78] R. Lomoth, P. Huang, J. T. Zheng, L. C. Sun, L. Hammarstrom, B. Åkermark, S. Styring, *Eur. J. Inorg. Chem.* **2002**, 1965.
[79] P. Huang, A. Magnuson, R. Lomoth, M. Abrahamsson, M. Tamm, L. Sun, B. van Rotterdam, J. Park, L. Hammarstrom, B. Åkermark, S. Styring, *J. Inorg. Biochem.* **2002**, 159.
[80] L. Hammarstrom, L. C. Sun, B. Åkermark, S. Styring, *Spectrochim. Acta Part A* **2001**, 2145.
[81] K. E. Berg, A. Tran, M. K. Raymond, M. Abrahamsson, J. Wolny, S. Redon, M. Andersson, L. C. Sun, S. Styring, L. Hammarstrom, H. Toftlund, B. Åkermark, *Eur. J. Inorg. Chem.* **2001**, 1019.
[82] N. S. Hush, *Coord. Chem. Rev.* **1985**, *64*, 135.
[83] N. S. Hush, *Prog. Inorg. Chem.* **1967**, *8*, 391.
[84] R. C. Rocha, H. E. Toma, *Polyhedron* **2002**, *21*, 2089.
[85] M. V. Russo, C. Lo Sterzo, P. Franceschini, G. Biagini, A. Furlani, *J. Organomet. Chem.* **2001**, *619*, 49.
[86] M. Carano, M. Careri, F. Cicogna, I. D'Ambra, J. L. Houben, G. Ingrosso, M. Marcaccio, F. Paolucci, C. Pinzino, S. Roffia, *Organometallics* **2001**, *20*, 3478.
[87] T. Weyland, K. Costuas, L. Toupet, J. F. Halet, C. Lapinte, *Organometallics* **2000**, *19*, 4228.
[88] M. Younus, N. J. Long, P. R. Raithby, J. Lewis, *J. Organomet. Chem.* **1998**, *570*, 55.
[89] N. Chanda, R. H. Laye, S. Chakraborty, R. L. Paul, J. C. Jefferey, M. D. Ward, G. K. Lahiri, *J. Chem. Soc. Dalton Trans.* **2002**, 3496.
[90] S. Chakraborty, R. H. Laye, P. Munshi, R. L. Paul, M. D. Ward, G. K. Lahiri, *J. Chem. Soc. Dalton Trans.* **2002**, 2348.
[91] B. Sarkar, R. H. Laye, B. Mondal, S. Chakraborty, R. L. Paul, J. C. Jeffery, V. G. Puranik, M. D. Ward, G. K. Lahiri, *J. Chem. Soc. Dalton Trans.* **2002**, 2097.
[92] M. B. Kassim, R. L. Paul, J. C. Jeffery, J. A. McCleverty, M. D. Ward, *Inorg. Chim. Acta* **2002**, *327*, 160.
[93] R. H. Laye, S. M. Couchman, M. D. Ward, *Inorg. Chem.* **2001**, *40*, 4089.
[94] A. Behrendt, S. M. Couchman, J. C. Jeffery, J. A. McCleverty, M. D. Ward, *J. Chem. Soc. Dalton Trans.* **1999**, 4349.
[95] N. C. Harden, E. R. Humphrey, J. C. Jeffery, S. M. Lee, M. Marcaccio, J. A. McCleverty, L. H. Rees, M. D. Ward, *J. Chem. Soc. Dalton Trans.* **1999**, 2417.
[96] T. Bartik, B. Bartik, M. Brady, R. Dembinski, J. A. Gladysz, *Angew. Chem.* **1996**, *108*, 467; *Angew. Chem. Int. Ed. Engl.* **1996**, *35*, 414.
[97] M. B. Robin, P. Day, *Adv. Inorg. Chem. Radiochem.* **1967**, *10*, 247.
[98] R. Das, K. K. Nanda, I. Paul, S. Baitalik, K. Nag, *Polyhedron* **1994**, *13*, 2639.
[99] T. Ise, T. Ishida, T. Nogami, *Mol. Cryst. Liq. Cryst.* **2002**, *379*, 147.
[100] J. S. Sun, H. H. Zhao, O. Y. Xiang, R. Clerac, J. A. Smith, J. M. Clemente-Juan, C. Gomez-Garcia, E. Coronado, K. R. Dunbar, *Inorg. Chem.* **1999**, *38*, 5841.
[101] STOE-IPDS software package, Version 2.87 5/1998, STOE&Cie, Darmstadt (Germany), **1998**.
[102] G. M. Sheldrick, *Acta Crystallogr. Sect. A* **1996**, *46*, 467.
[103] G. M. Sheldrick, SHELXL-97, Program for refinement of crystal structures; University of Göttingen (Germany), **1997**.
[104] A. L. Spek, PLATON-91, A computer program for the graphical representation of crystallographic models, University of Utrecht (The Netherlands), **1991**.
[105] H. D. Flack, *Acta Crystallogr. Sect. A* **1983**, *39*, 876.
[106] H. D. Flack, G. Bernardinelli, *J. Appl. Crystallogr.* **2000**, *33*, 1143.
[107] ADF2002.02, *SCM*, Theoretical Chemistry, Vrije Universiteit, Amsterdam (The Netherlands), http://www.scm.com; a) G. te Velde, F. M. Bickelhaupt, E. J. Baerends, C. F. Guerra, S. J. A. Van Gisbergen, J. G. Snijders, T. Ziegler, *J. Comput. Chem.* **2001**, *22*, 931; b) C. F. Guerra, J. G. Snijders, G. te Velde, E. J. Baerends, *Theor. Chem. Acc.* **1998**, *99*, 391.
[108] S. H. Vosko, L. Wilk, M. Nusair, *Can. J. Phys.* **1980**, *58*, 1200.
[109] A. D. Becke, *Phys. Rev. A* **1988**, *38*, 3098.
[110] a) J. P. Perdew, *Phys. Rev. B* **1986**, *33*, 8822; b) J. P. Perdew, *Phys. Rev. B* **1986**, *34*, 7406.
[111] G. te Velde, E. J. Baerends, *J. Comput. Chem.* **1992**, *99*, 84.
[112] A. Klamt, G. Schüürmann, *J. Chem. Soc. Perkin Trans. 2* **1993**, 799.
[113] C. C. Pye, T. Ziegler, *Theor. Chem. Acc.* **1999**, *101*, 396.

Received: June 20, 2003 [F5254]